

Supporting Information

Supramolecular effect of aromaticity on the crystal packing of Furan/Thiophene carboxamide compounds

Maryam Rahmani^a, Alireza Salimi*^a, Somayeh Mohammadzadeh^a, Hazel A. Sparkes^b

^aDepartment of Chemistry, Ferdowsi University of Mashhad, 917791436, Mashhad, Iran

^bSchool of Chemistry, University of Bristol, Cantock's Close, Bristol, BS8 1TS, UK

Contents:

- 1) The Cambridge Structural Database (CSD) analysis of C-H... π interactions in five-membered furan ring, Page S3
- 2) The Cambridge Structural Database (CSD) analysis of π ... π interactions between furan rings (π_{Furan} ... π_{Furan} interaction), Page S8
- 3) The Cambridge Structural Database (CSD) analysis of π ... π interactions between pyrazine rings (π_{pyz} ... π_{pyz} interaction), Page S11
- 4) The Cambridge Structural Database (CSD) analysis of π ... π interactions between thiophene rings (π_{Thio} ... π_{Thio} interaction), Page S14
- 5) NMR and IR data of *I*, Page S18
- 6) NMR and IR data of *II*, Page S121
- 7) Figure S21. Independent view of titled compounds by two probable conformations for five-membered heterocyclic rings. The agreement with experimental result has been presented by thick mark. Page S25

- 8) Figure S22. Representation of the most stable tetramer motifs of *I* which are labeled based on the interaction energy ranking. Page S34
- 9) Figure S23. Representation of the most stable tetramer motifs of *II* which are labeled based on the interaction energy ranking. Page S45
- 10) Table S1. The binding energy (E_{calc} in kJ/mol) of the most stable tetramer fragments of compound *I*, along with contribution of cooperativity (E_{coop}), HB (E_{HB}) and $\pi \dots \pi$ stacking ($E_{\pi \dots \pi}$) energies as the magnitude (in kJ/mol) and percentage of total binding energy, as well as their weighted contributions. Page S46
- 11) Table S2. The binding energy (E_{calc} in kJ/mol) of the most stable tetramer fragments of compound *II*, along with contribution of cooperativity (E_{coop}), HB (E_{HB}) and $\pi \dots \pi$ stacking ($E_{\pi \dots \pi}$) energies as the magnitude (in kJ/mol) and percentage of total binding energy, as well as their weighted contributions. Page S47

1) The Cambridge Structural Database (CSD) analysis of C-H... π interactions in five-membered furan ring

The Cambridge Structural Database (CSD) search was carried out with help of Vista program (version 2.1) in the November 2013 release of the CSD version 5.35. The searches based on geometrical parameters of the H...Cg contact distance (d_{cent}), H...Pln(mean plane) distance (d_{pln}), C-H...Cg angle ($\alpha/^\circ$) and the displacement angle ($\beta/^\circ$) for CH... π interactions of furan ring are shown in Figures S1-S4. The Scattergrams for a correlation between d_{cent} /alpha angle and d_{pln} /alpha angle are depicted in Figure S5.

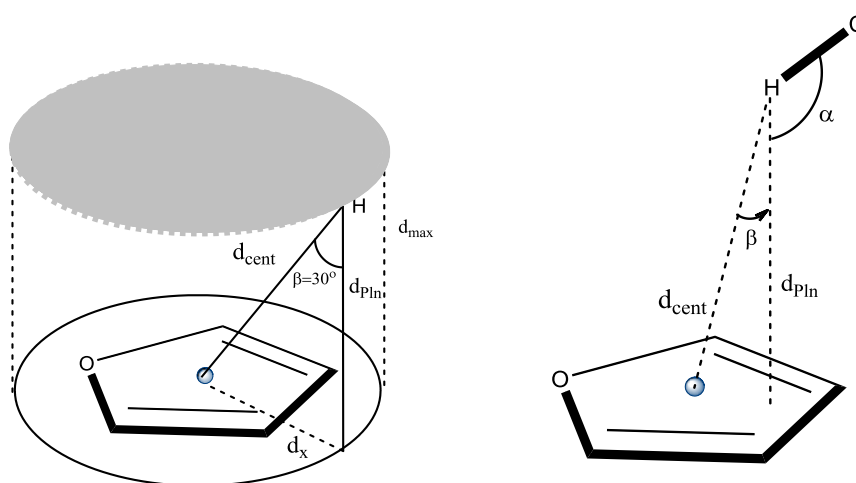


Figure S1. Representation of geometrical parameters related to CH... π interactions of furan ring in the database analysis. The restricted parameters are $0 < \beta < 30^\circ$ and $d_{\text{pln}} = d_{\text{max}} = 4.0 \text{ \AA}$ in which $d_x = 2 \text{ \AA}$ referred to the maximum radius of cylindrical space searchable.

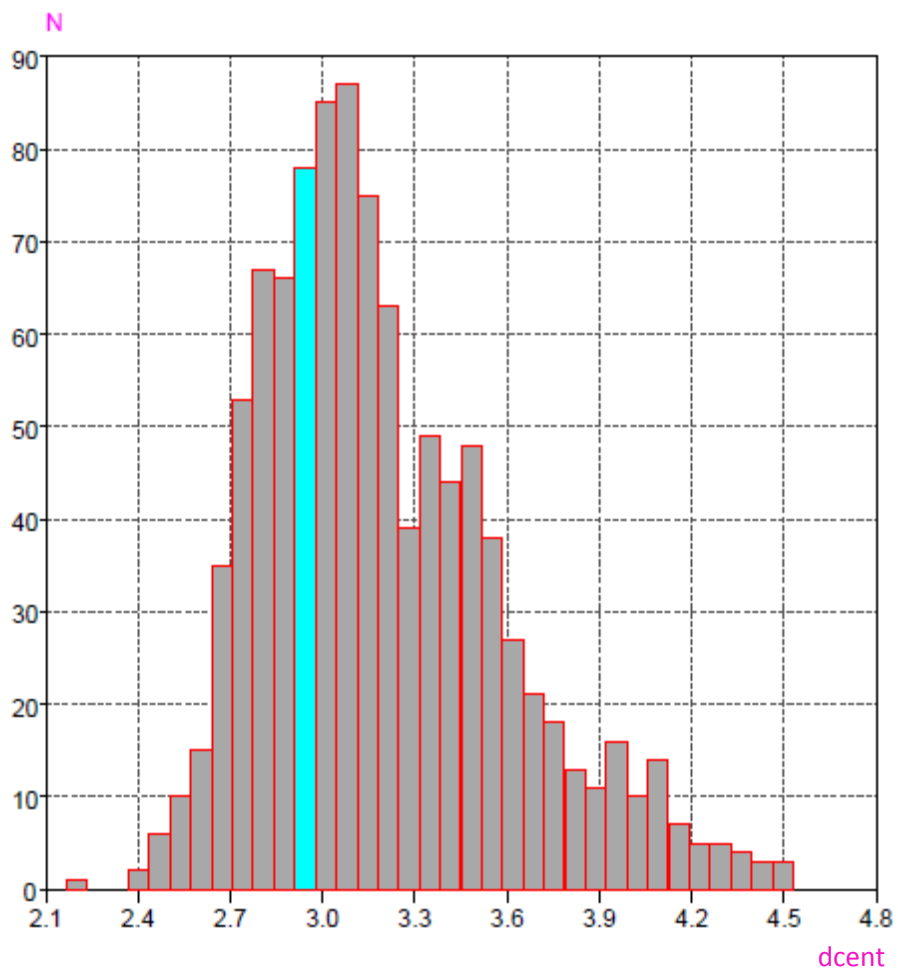


Figure S2. The Histogram for the H...Cg contact distance (d_{cent}), from a CSD search (592 hits) which was obtained between 2.1 Å to 4.5 Å. The blue column is related to the value of C9-H9... π_{Furan} interaction in compound I^{Furan} .

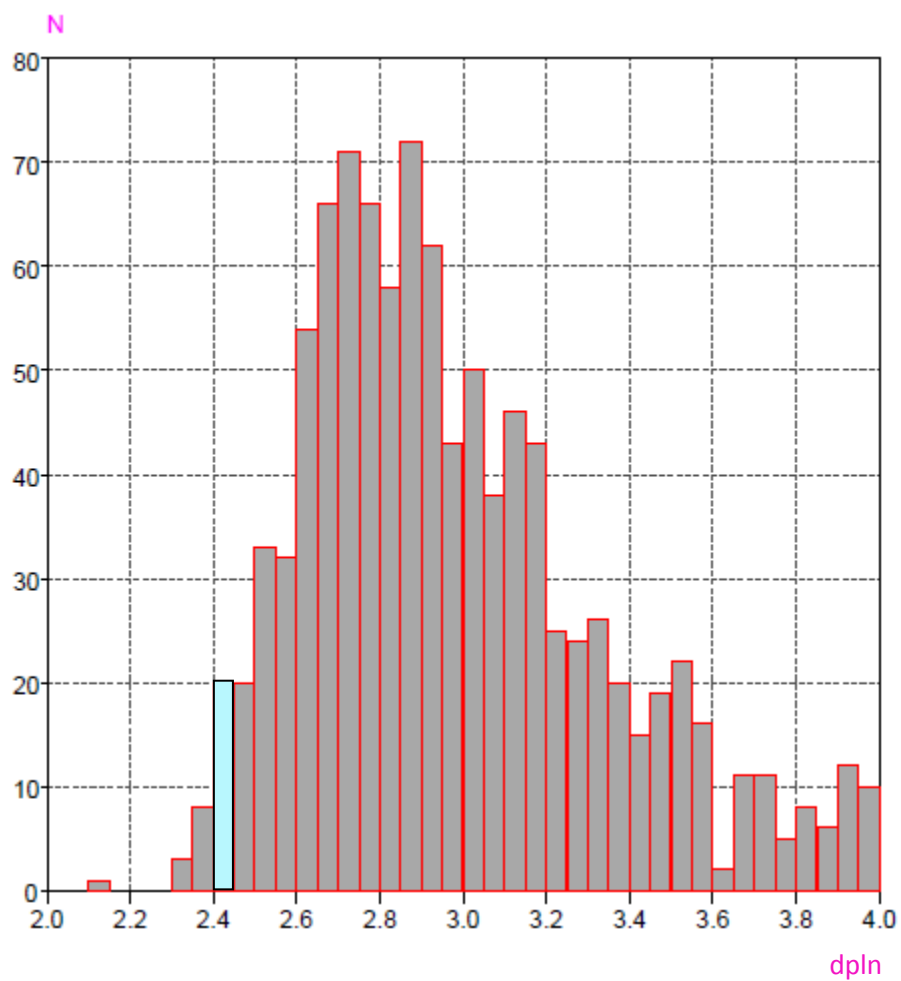


Figure S3. The Histogram for the H...Pln (mean plane) distance (d_{pln}) from a CSD search (592 hits) which was constrained between 2.0 \AA and 4.0 \AA .

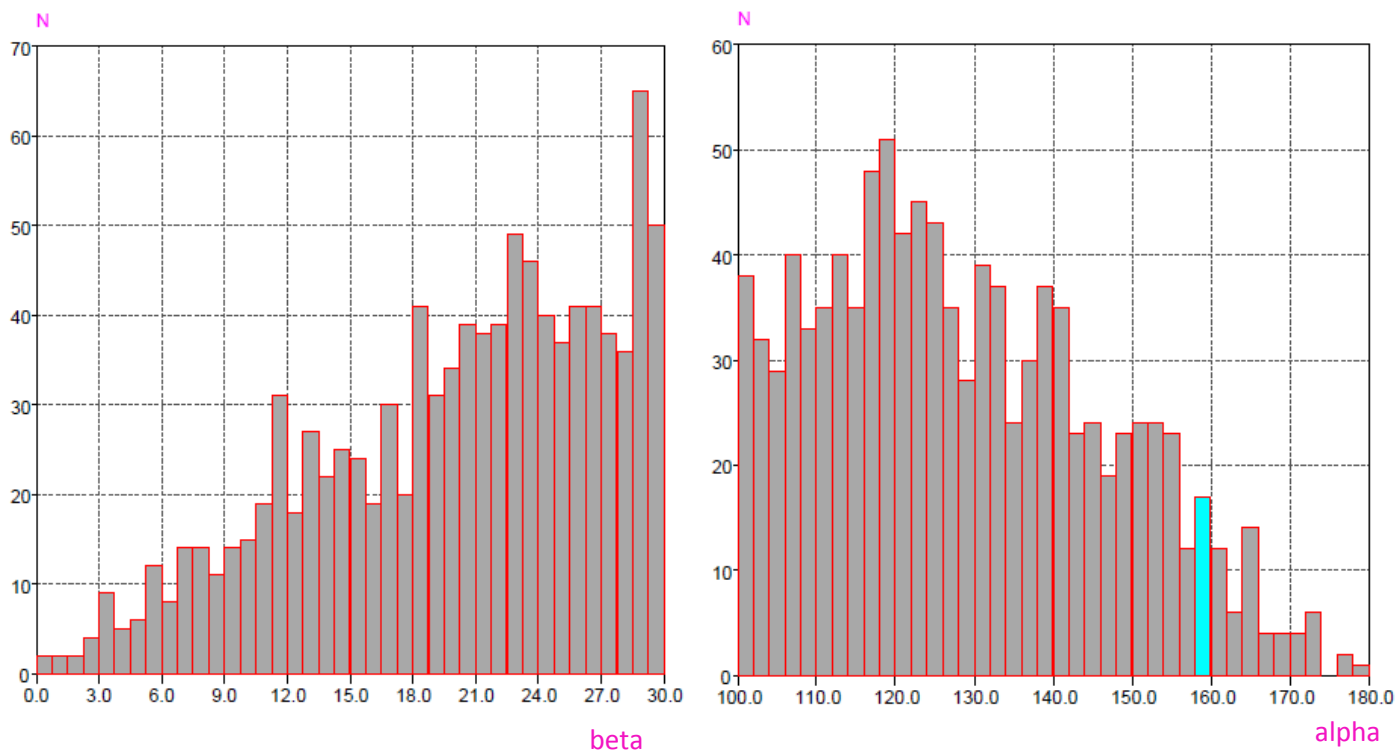


Figure S4. The Histograms for the C-H...Cg angle (α /°) and the displacement angle (β /°) for CH... π interactions of furan ring from a CSD search (592 hits) which was constrained for α between 100° and 180° and for β between 0° and 30°.

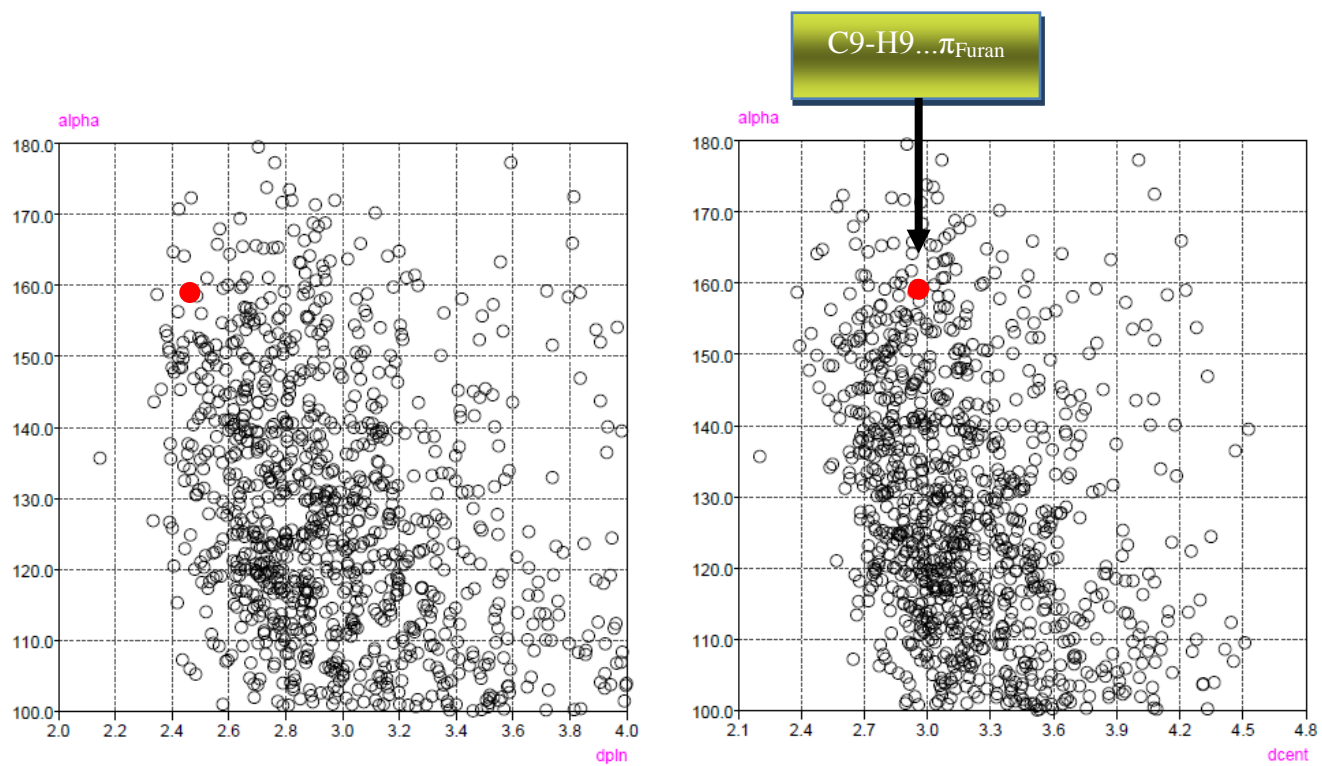


Figure S5. The Scattergrams for a correlation between d_{cent}/α angle (right) and d_{pln}/α angle (left). The red spots are related to the corresponding values of C9-H9... π_{Furan} interaction in compound I^{Furan} .

2) The Cambridge Structural Database (CSD) analysis of $\pi \cdots \pi$ interactions between furan rings ($\pi_{\text{Furan}} \cdots \pi_{\text{Furan}}$ interaction)

The Cambridge Structural Database (CSD) search was carried out with help of Vista program (version 2.1) in the November 2013 release of the CSD version 5.35. The searches based on geometrical parameters of the centroid–centroid distance (C–C/Å) and the displacement angle (P–CC/°) for $\pi \cdots \pi$ interactions between furan rings ($\pi_{\text{Furan}} \cdots \pi_{\text{Furan}}$ interaction) are shown in Figures S6 and S7. The Scattergram for a correlation between the centroid–centroid distance (C–C/Å) and the displacement angle (P–CC/°) of five memebred furan rings is depicted in Figure S8.

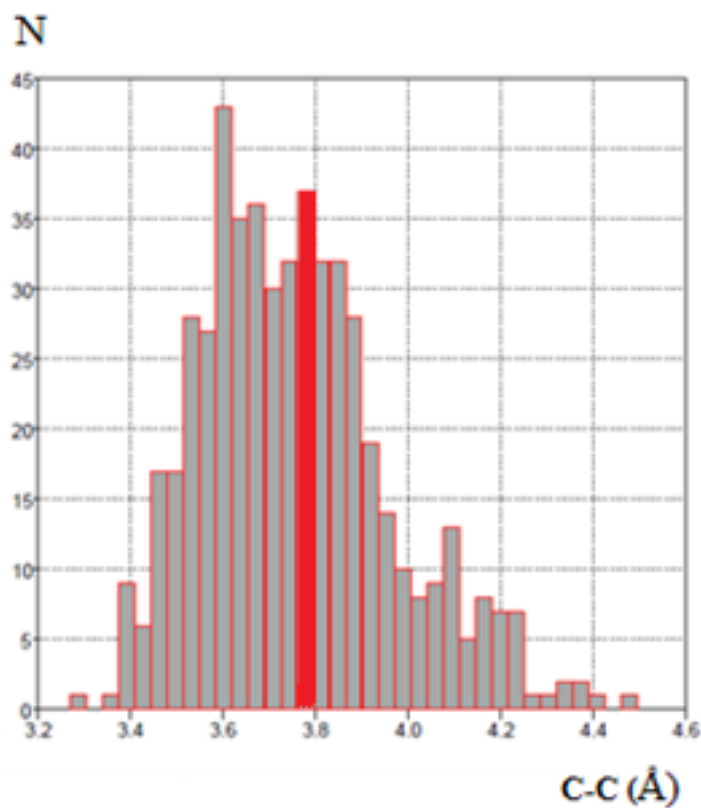


Figure S6. The Histogram for the centroid–centroid distance (C–C/Å) between furan rings from a CSD search (519 hits) which was constrained between 3.2 Å and 4.6 Å. The red column is related to the value of $\pi_{\text{Furan}} \cdots \pi_{\text{Furan}}$ interaction in compound I^{Furan} .

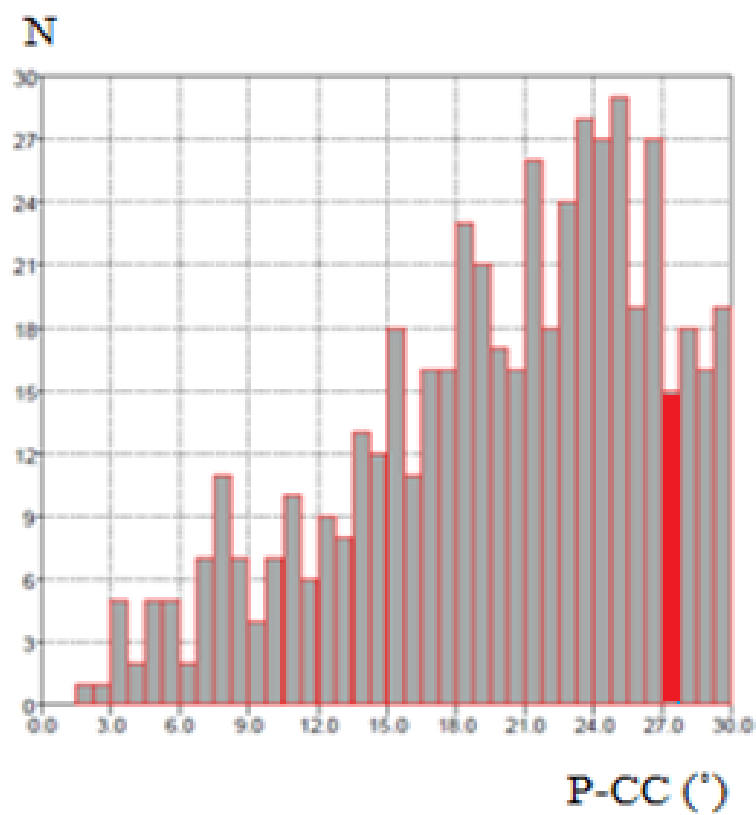


Figure S7. The Histogram for the displacement angle (P-CC/°) between furan rings from a CSD search (519 hits) which was constrained between 0° and 30°. The red column is related to the value of $\pi_{\text{Furan}} \cdots \pi_{\text{Furan}}$ interaction in compound I^{Furan} .

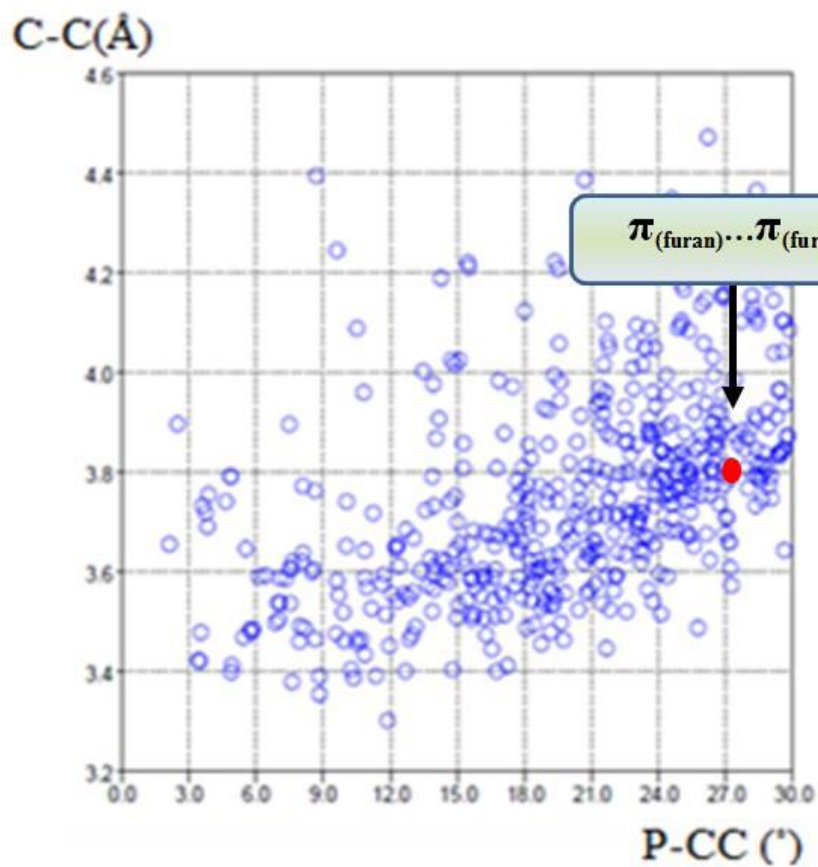


Figure S8. The Scattergram for a correlation between the centroid–centroid distance (C–C/Å) and the displacement angle (P–CC/°). The red spot is related to the corresponding values of $\pi_{\text{Furan}} \cdots \pi_{\text{Furan}}$ interaction in compound I^{Furan} .

3) The Cambridge Structural Database (CSD) analysis of $\pi\cdots\pi$ interactions between pyrazine rings ($\pi_{\text{pyz}}\cdots\pi_{\text{pyz}}$ interaction)

The searches based on geometrical parameters of the centroid–centroid distance (C–C/Å) and the displacement angle (P–CC/°) for $\pi\cdots\pi$ interactions between pyrazine rings ($\pi_{\text{Furan}}\cdots\pi_{\text{Furan}}$ interaction) are shown in Figures S9 and S10. The Scattergram for a correlation between the centroid–centroid distance (C–C/Å) and the displacement angle (P–CC/°) of six memebred pyrazine rings is depicted in Figure S11.

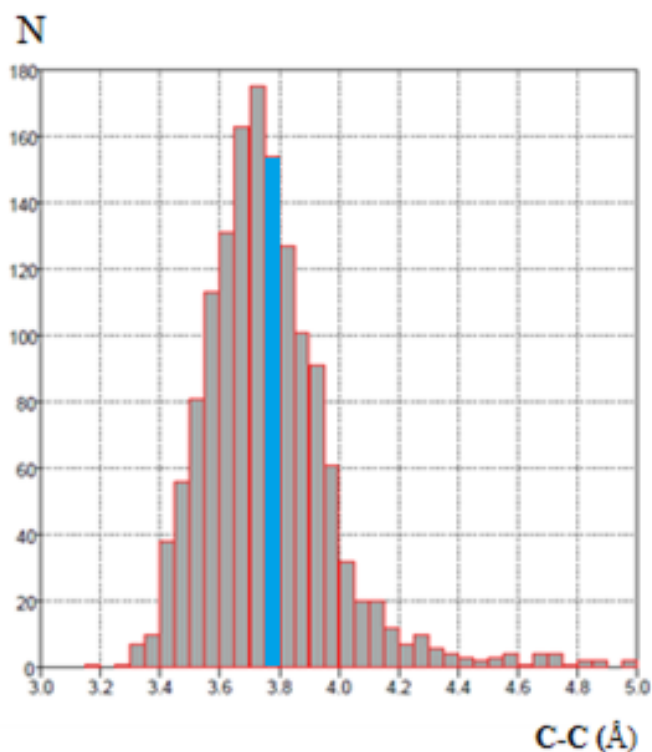


Figure S9. The Histogram for the centroid–centroid distance (C–C/Å) between pyrazine rings from a CSD search (1449 hits) which was constrained between 3.0 Å and 5.0 Å. The blue column is related to the value of $\pi_{\text{pyz}}\cdots\pi_{\text{pyz}}$ interaction in compound I^{Furan} .

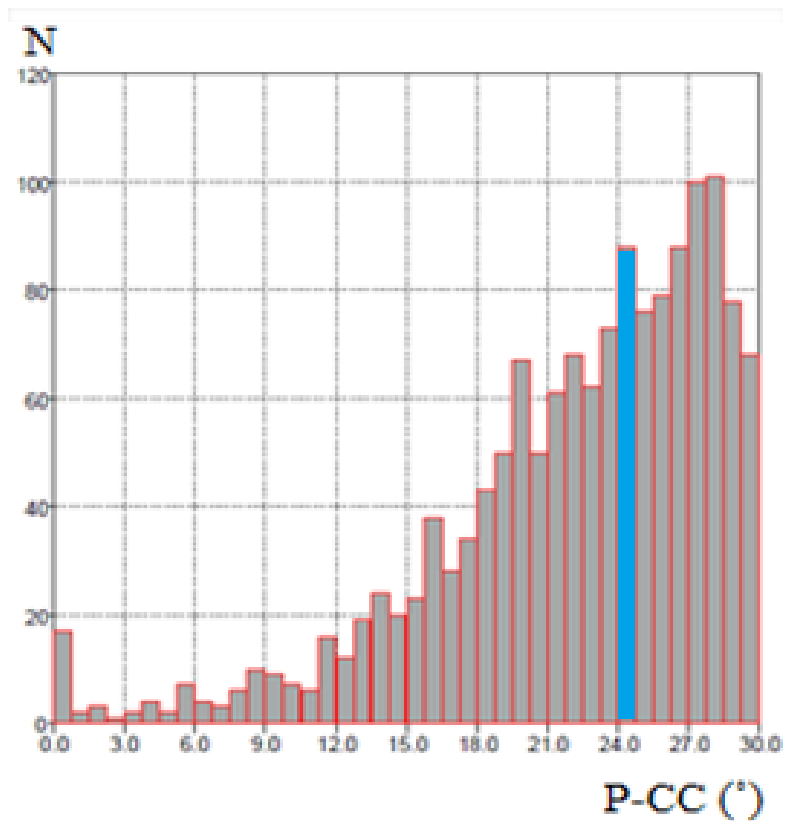


Figure S10. The Histogram for the displacement angle (P-CC/°) between pyrazine rings from a CSD search (1449 hits) which was constrained between 0° and 30°. The blue column is related to the value of $\pi_{\text{pyz}} \cdots \pi_{\text{pyz}}$ interaction in compound I^{Furan} .

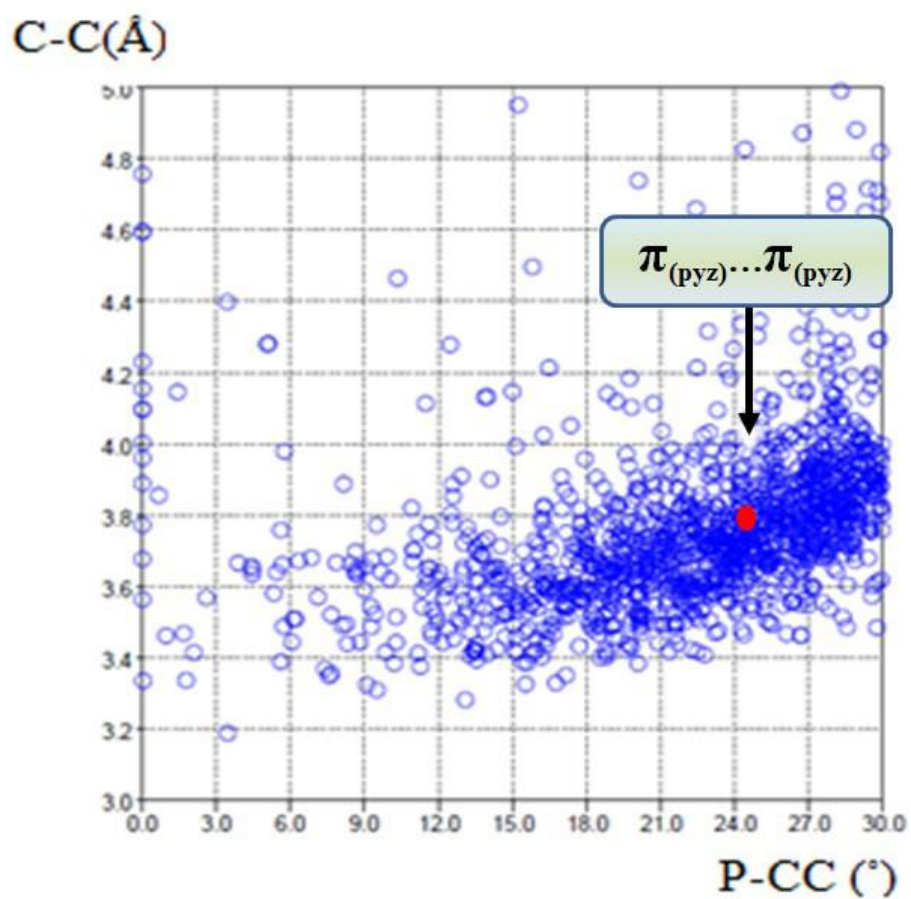


Figure S11. The Scattergram for a correlation between the centroid–centroid distance (C–C/Å) and the displacement angle (P–CC/°). The red spot is related to the corresponding values of $\pi_{\text{pyz}} \cdots \pi_{\text{pyz}}$ interaction in compound I^{Furan} .

4) The Cambridge Structural Database (CSD) analysis of $\pi\cdots\pi$ interactions between thiophene rings ($\pi_{\text{Thio}}\cdots\pi_{\text{Thio}}$ interaction)

The searches based on geometrical parameters of the centroid–centroid distance (C–C/Å) and the displacement angle (P–CC/°) for $\pi\cdots\pi$ interactions between thiophene rings ($\pi_{\text{Thio}}\cdots\pi_{\text{Thio}}$ interaction) are shown in Figures S12 and S13. The Scattergram for a correlation between the centroid–centroid distance (C–C/Å) and the displacement angle (P–CC/°) of five memebred thiophene rings is depicted in Figure S14.

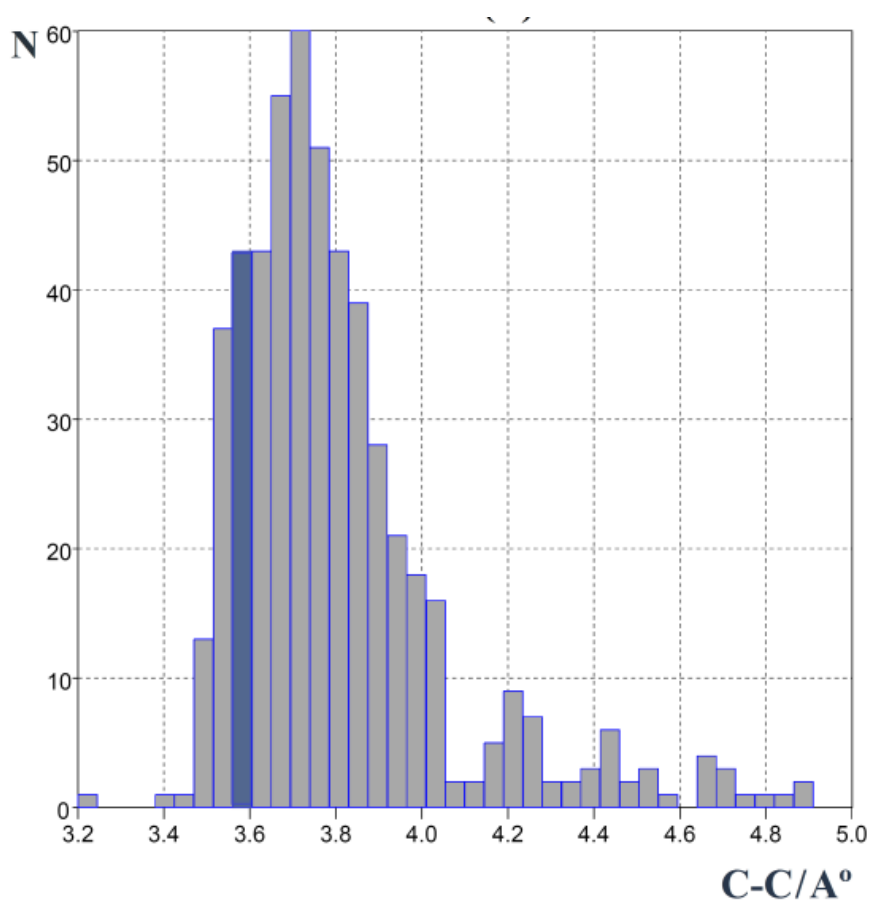


Figure S12. The Histogram for the centroid–centroid distance (C–C/Å) between thiophene rings from a CSD search (526 hits) which was constrained between 3.2 Å and 5.0 Å. The blue column is related to the value of $\pi_{\text{Thio}}\cdots\pi_{\text{Thio}}$ interaction in compound II^{Thiophene}.

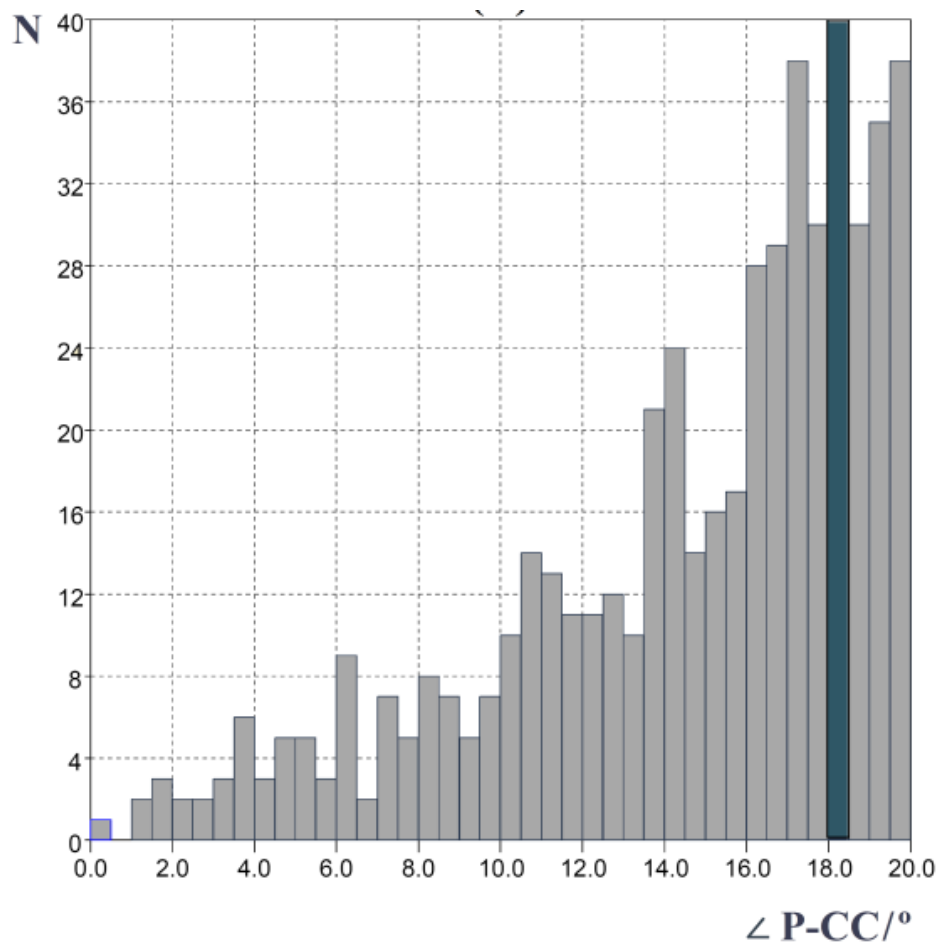


Figure S13. The Histogram for the displacement angle (P-CC/°) between thiophene rings from a CSD search (526 hits) which was constrained between 0° and 20°. The blue column is related to the value of $\pi_{\text{Thio}} \cdots \pi_{\text{Thio}}$ interaction in compound II^{Thiophene}.

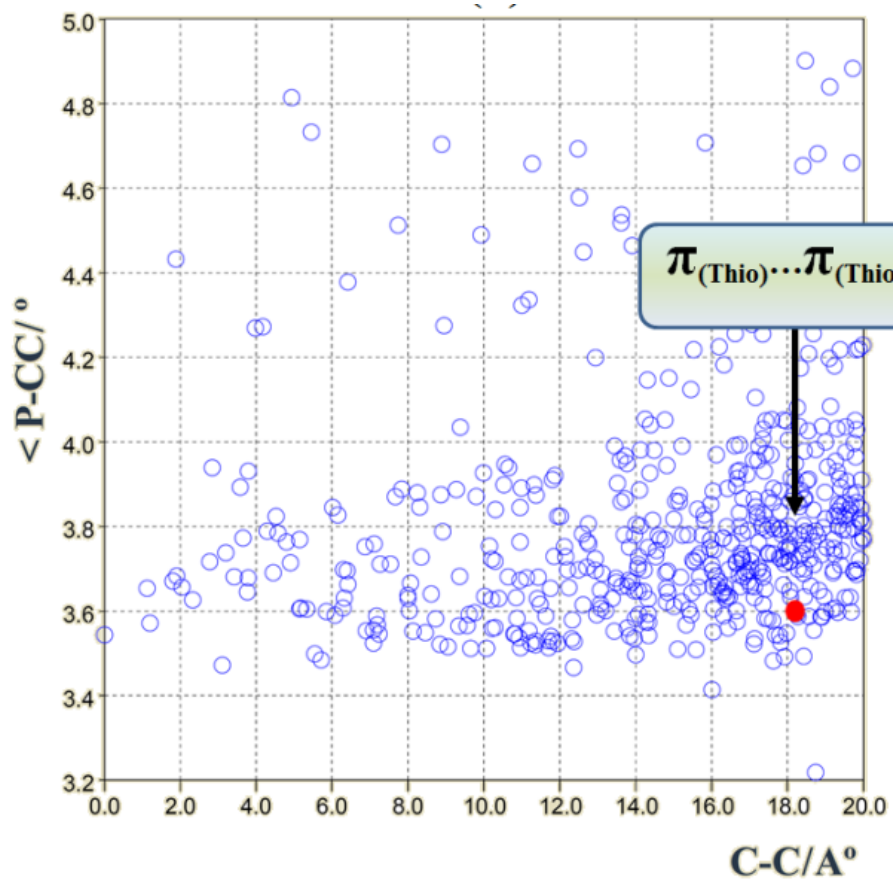


Figure S14. The Scattergram for a correlation between the centroid–centroid distance (C–C/A°) and the displacement angle (P–CC/°). The red spot is related to the corresponding values of $\pi_{\text{Thio}} \cdots \pi_{\text{Thio}}$ interaction in compound *II*^{Thiophene}.

5) NMR and IR data of *I*

^1H NMR (400 MHz, CDCl_3): δ 9.68 (d, $J=1.6$ Hz, 1*H*-pyrazine), 8.74 (s, 1*H*-Amide), 8.40 (d, $J=2.4$ Hz, 1*H*-pyrazine), 8.31 (dd, $J=1.6, 0.8$ Hz, 1*H*-pyrazine), 7.59 (dd, $J=0.8, 0.4$ Hz, 1*H*-furan), 7.35 (dd, $J=2.8, 0.8$ Hz, 1*H*-furan), 6.62 (dd, $J=2.0, 1.6$ Hz, 1*H*-furan). ^{13}C NMR (100.61 MHz, CDCl_3): δ 155.81 (C=O), 147.85 (C4-furan), 146.77 (C6-pyrazine), 145.16 (C1-furan), 142.23 (C9-pyrazine), 140.45 (C7-pyrazine), 137.11 (C8-pyrazine), 116.77 (C3-furan), 112.96 (C2-furan). Selected IR bands (KBr pellet, cm^{-1}): 3225 (b), 3124 (b), 1671 (s), 1545 (s), 1416 (s), 1307 (s), 723 (b).

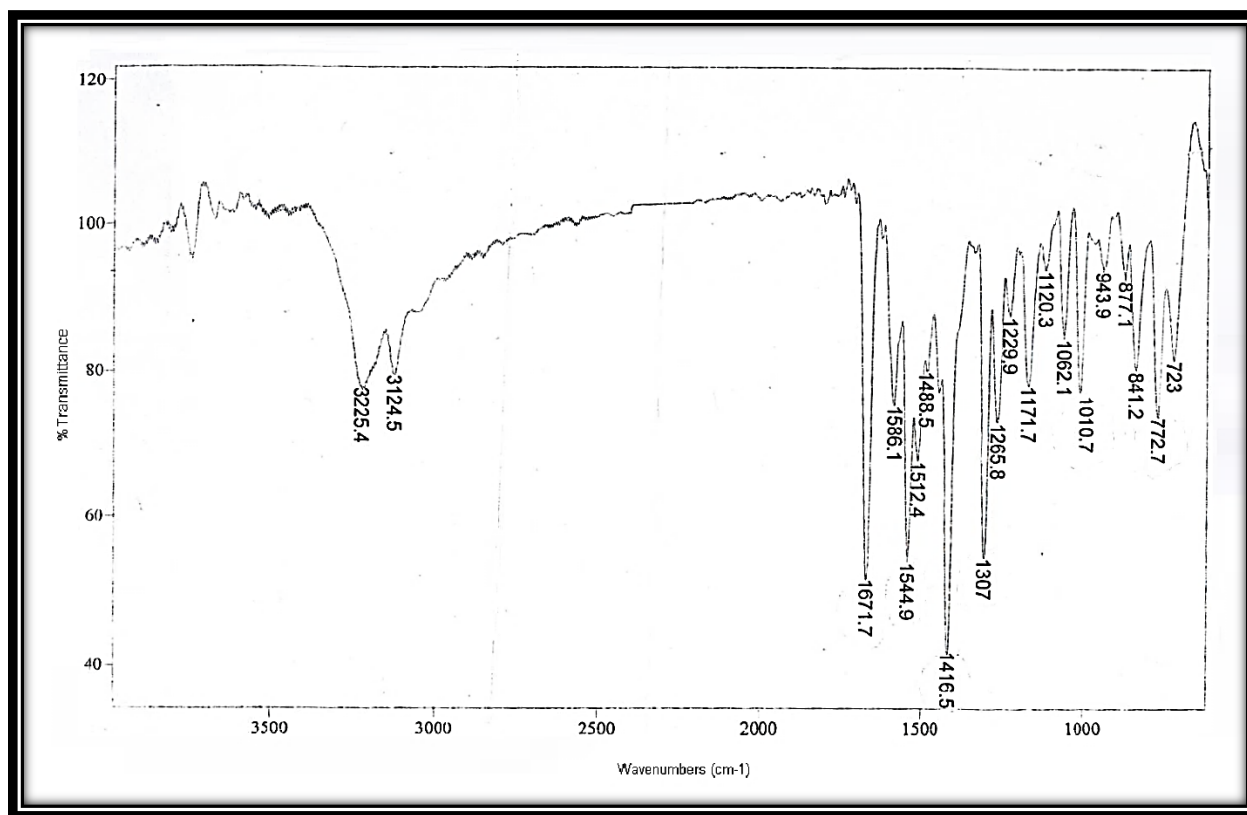


Figure S15. IR spectrum of *I*

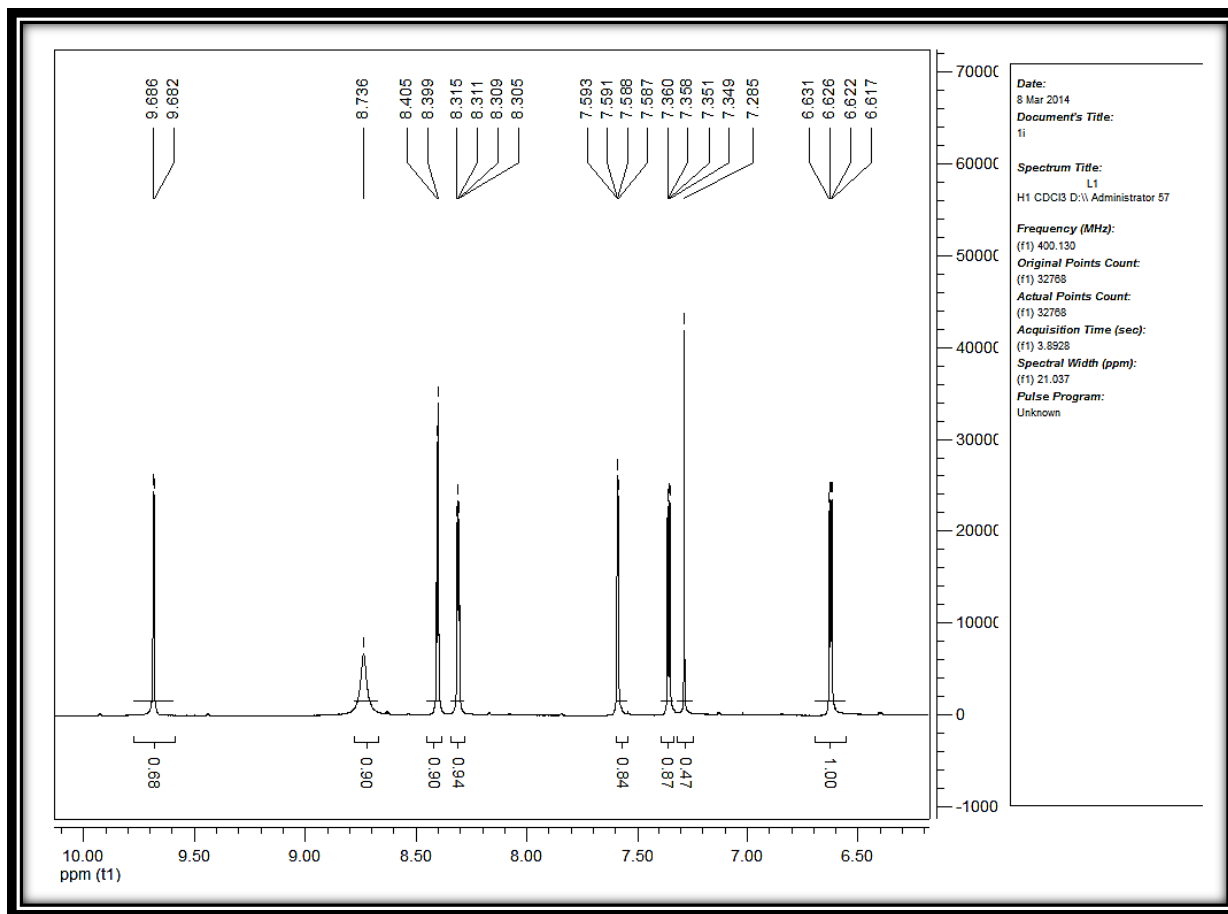


Figure S16.1H-NMR spectrum of I

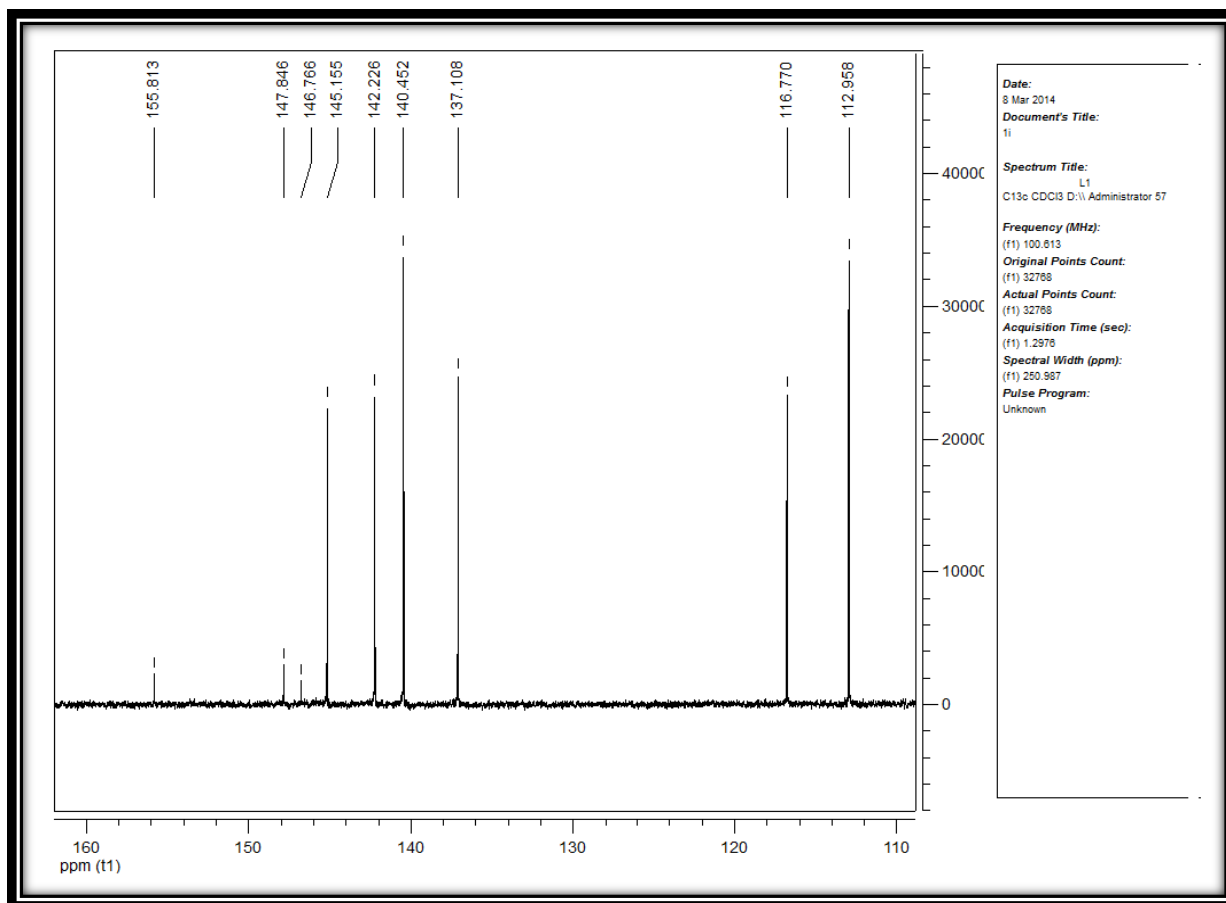


Figure S17.13C-NMR spectrum of I

6) NMR and IR data of II

^1H NMR (400 MHz, CDCl_3): δ 9.69 (s, 1*H*-pyrazine), 8.71 (s, 1*H*-Amide), 8.40 (d, $J=1.6$ Hz, 1*H*-pyrazine), 8.28 (s, 1*H*-pyrazine), 7.78 (dd, $J=3.2, 0.8$ Hz, 1*H*-thiophene), 7.66 (d, $J=4.4$ Hz, 1*H*-thiophene), 7.18 (d, $J=4.4$ Hz, 1*H*-thiophene). ^{13}C NMR (100.61 MHz, CDCl_3): δ 159.93 (C=O), 148.15 (C6-pyrazine), 141.99 (C4-furan), 140.31 (C9-pyrazine), 137.92 (C7-pyrazine), 137.39 (C8-pyrazine), 132.42 (C3-furan), 129.73 (C1-furan), 128.19 (C2-furan). Selected IR bands (KBr pellet, cm^{-1}): 3215 (b), 3084 (b), 1653 (s), 1536 (s), 1411 (s), 1299 (s), 735 (b).

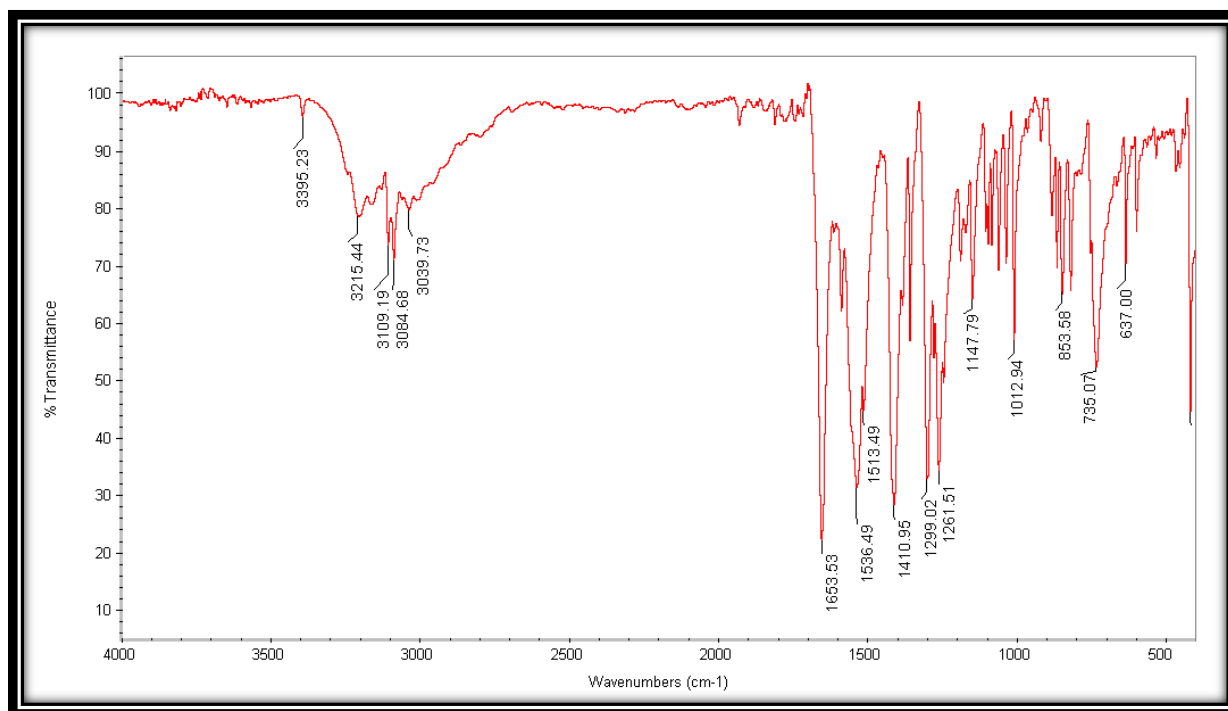


Figure S18. IR spectrum of II

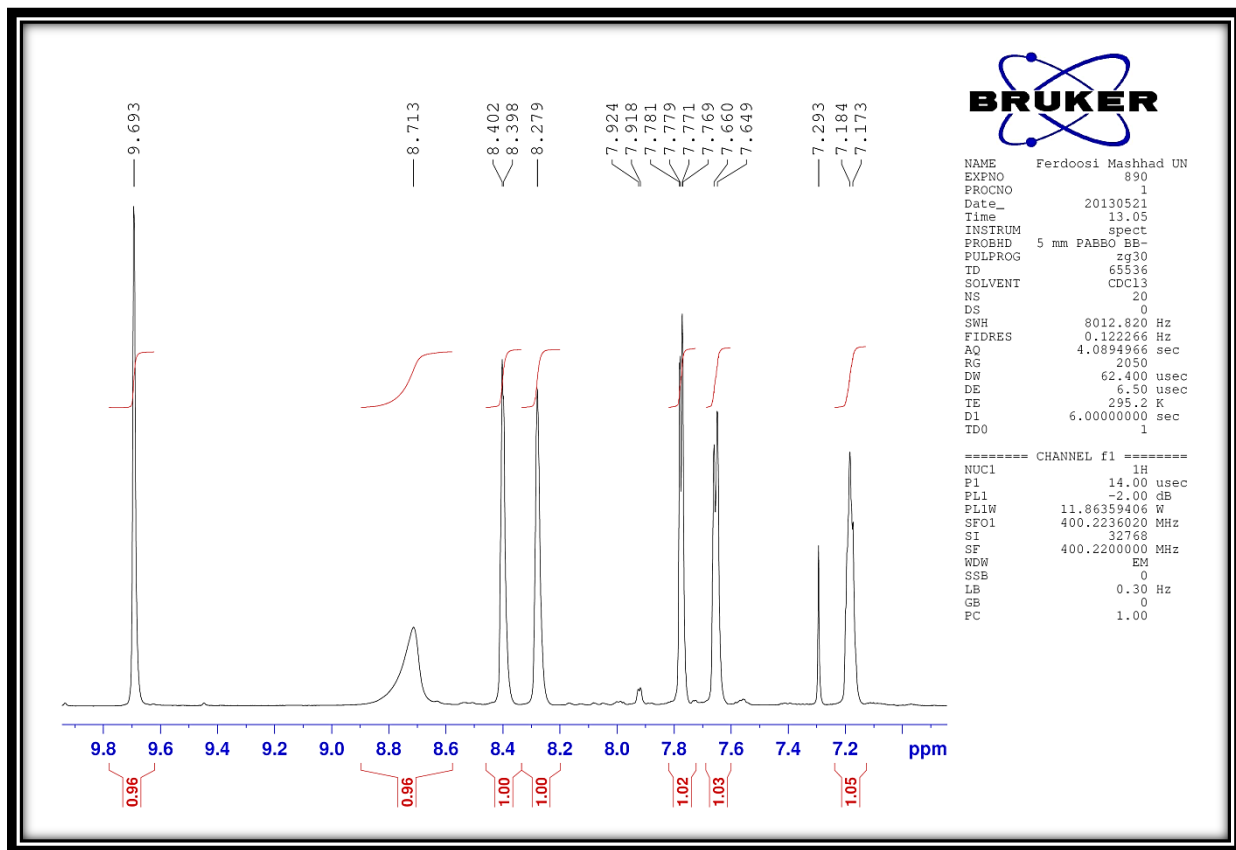


Figure S19. $^1\text{H-NMR}$ spectrum of II

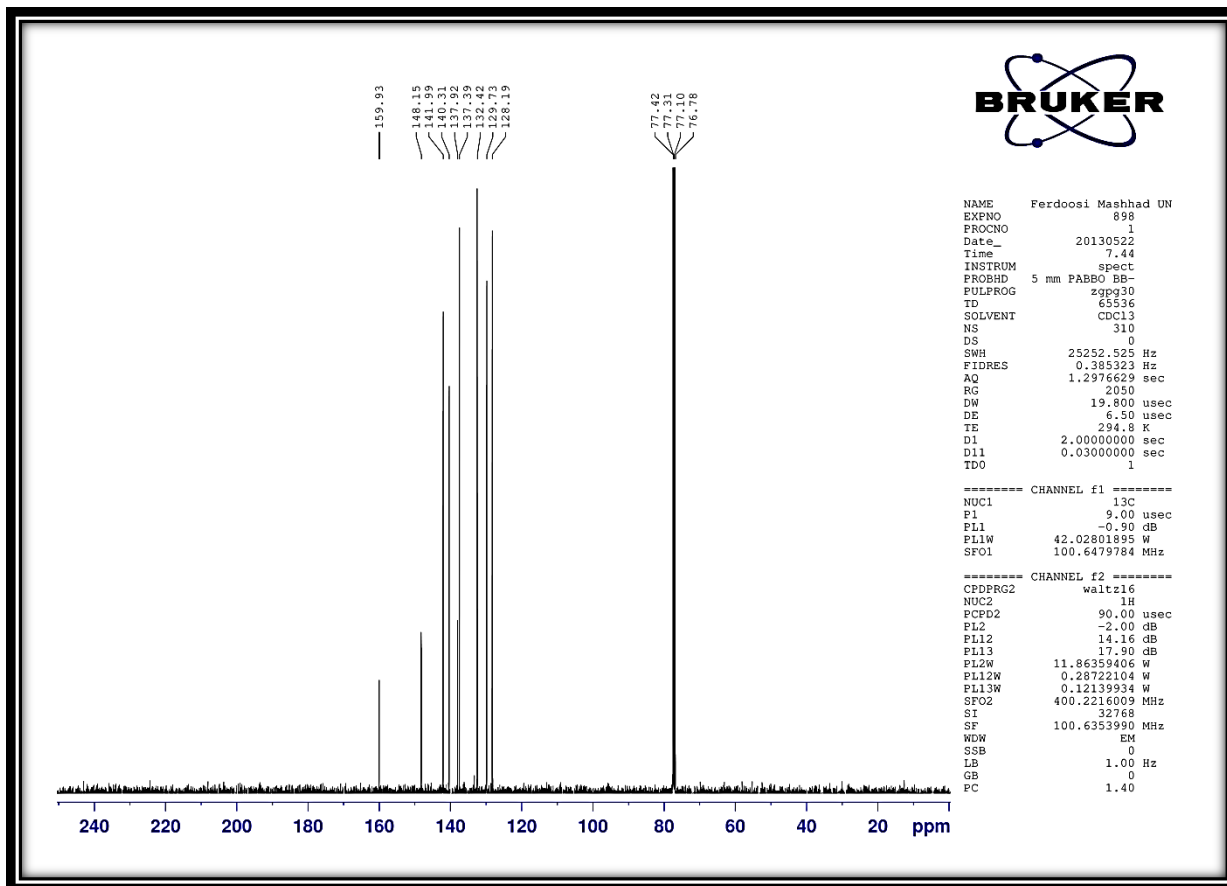


Figure S20.13C-¹³C-NMR spectrum of II

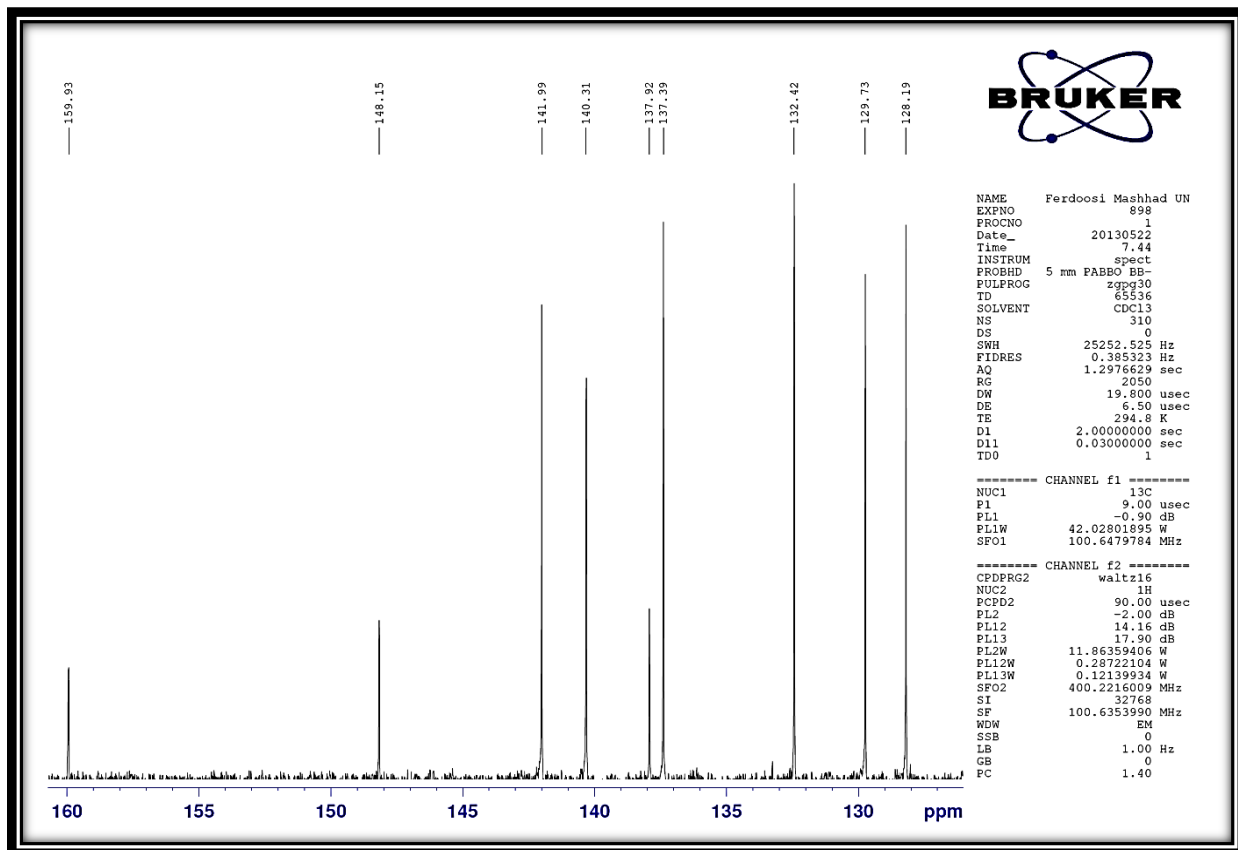


Figure S20.Extended ¹³C-NMR spectrum of II

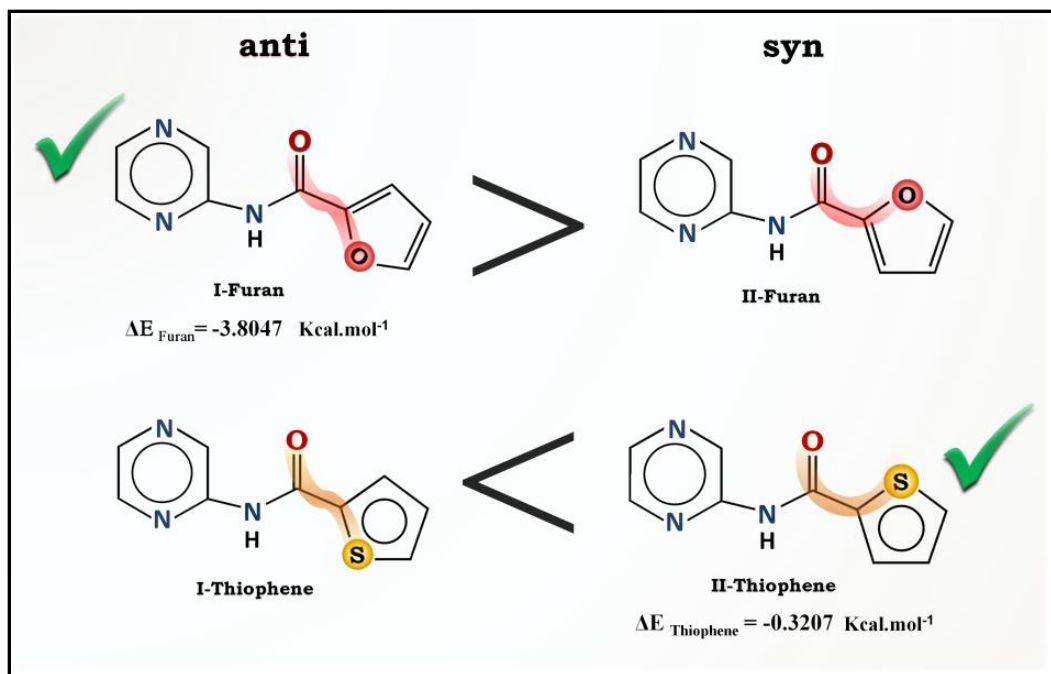
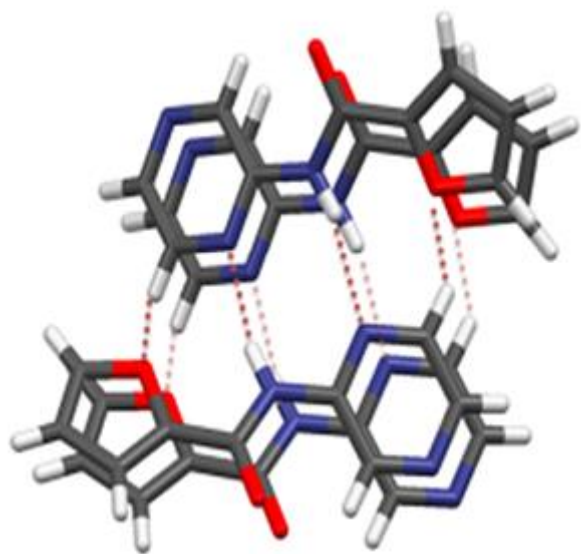
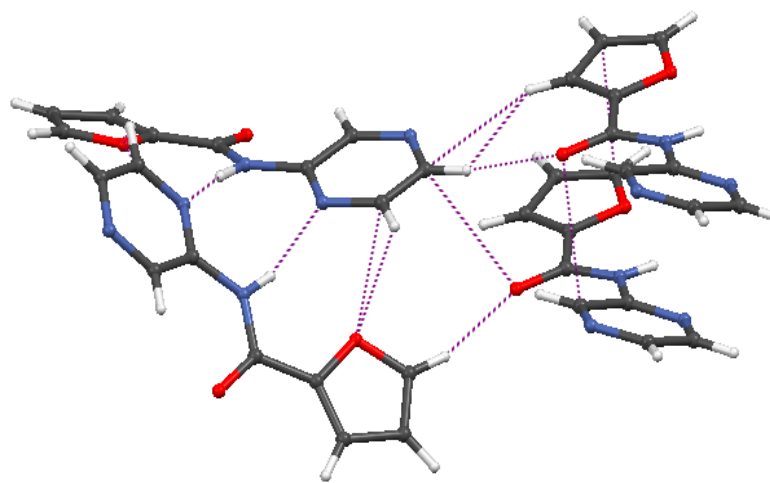


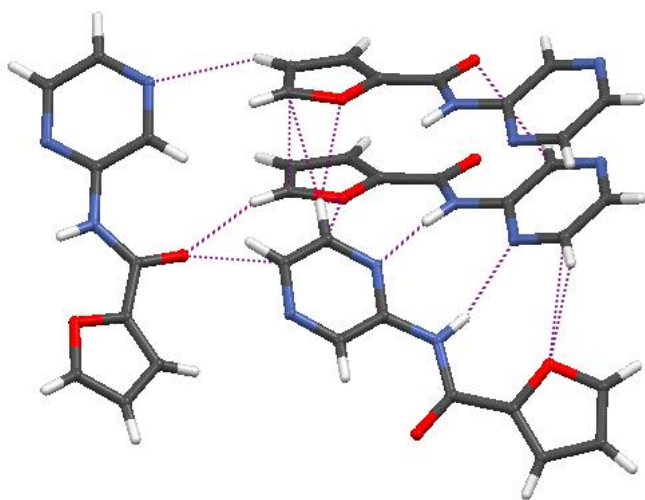
Figure S21. Independent view of titled compounds by two probable conformations for five-membered heterocyclic rings. The agreement with experimental result has been presented by thick mark.



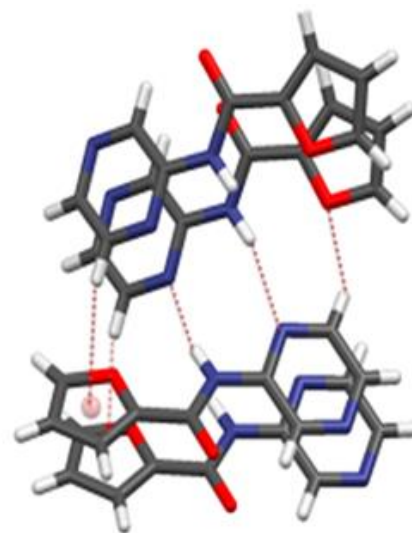
Tet 1



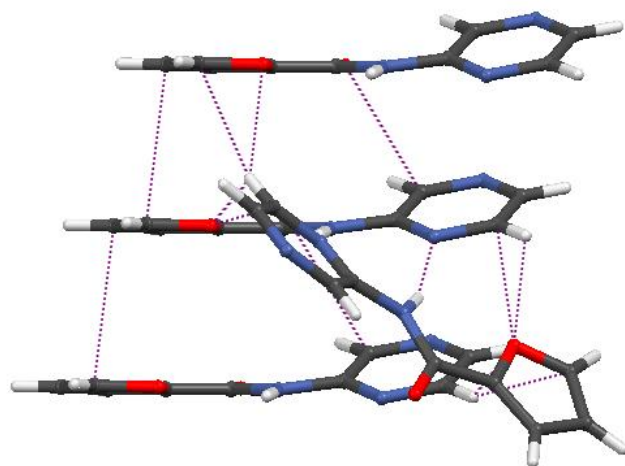
Tet 1



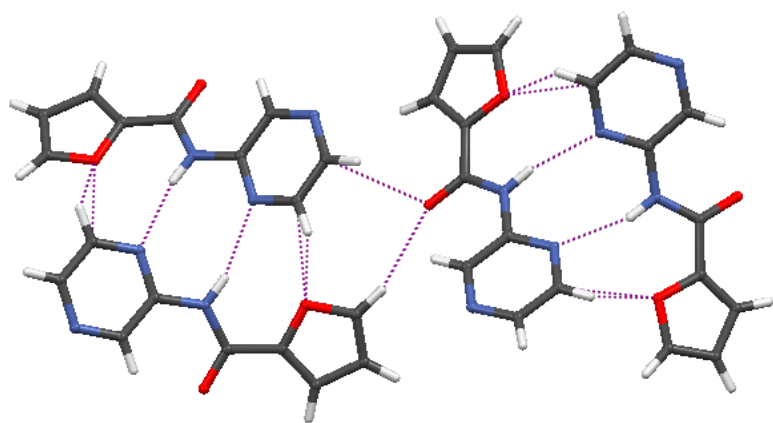
Tet 3



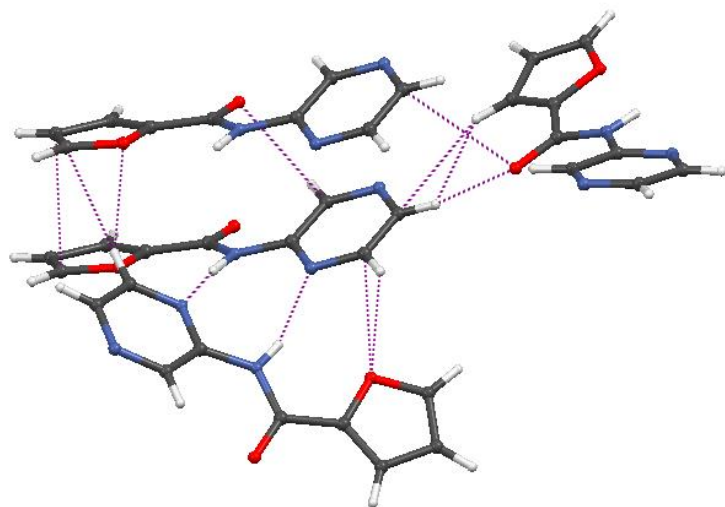
Tet 4



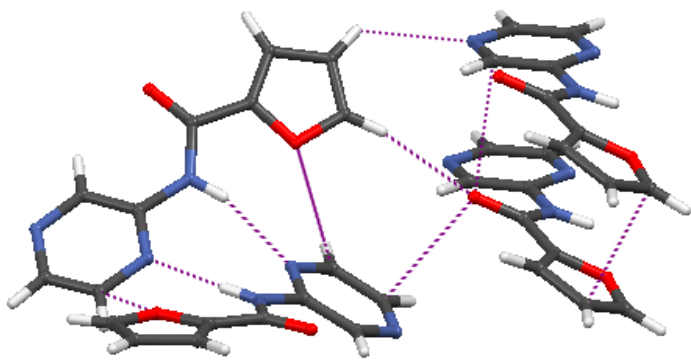
Tet 5



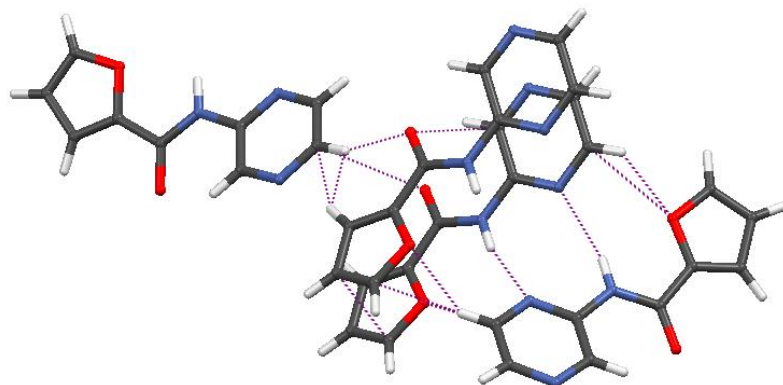
Tet 6



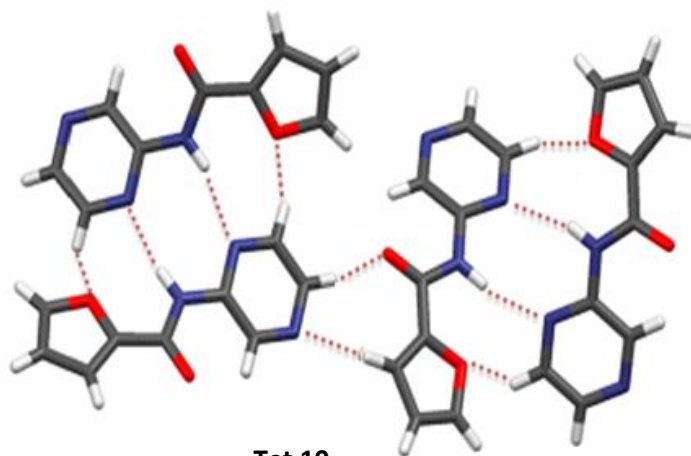
Tet 7



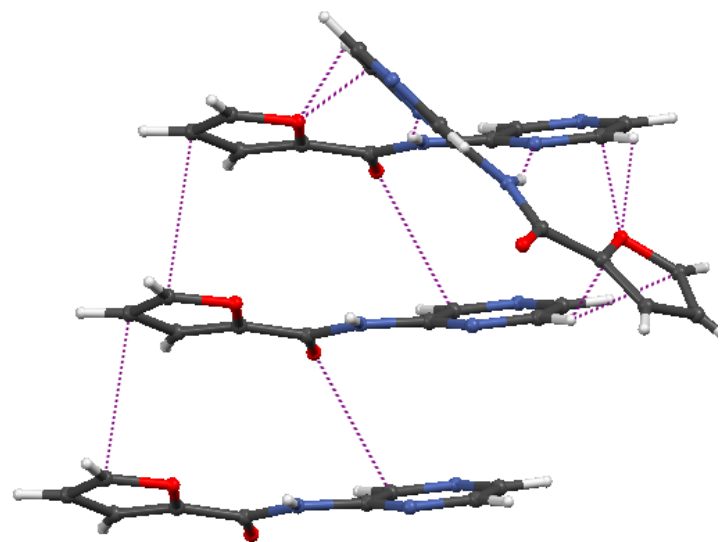
Tet 8



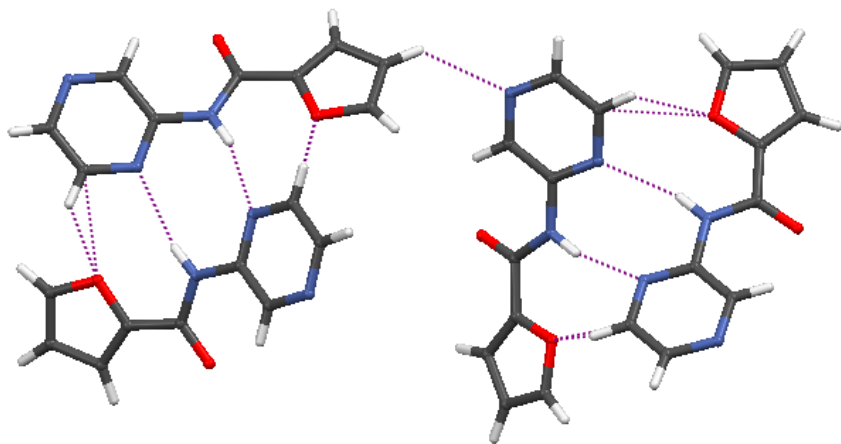
Tet 9



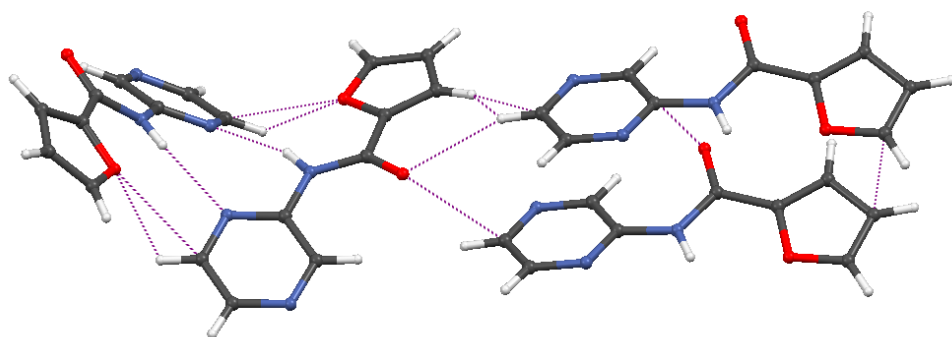
Tet 10



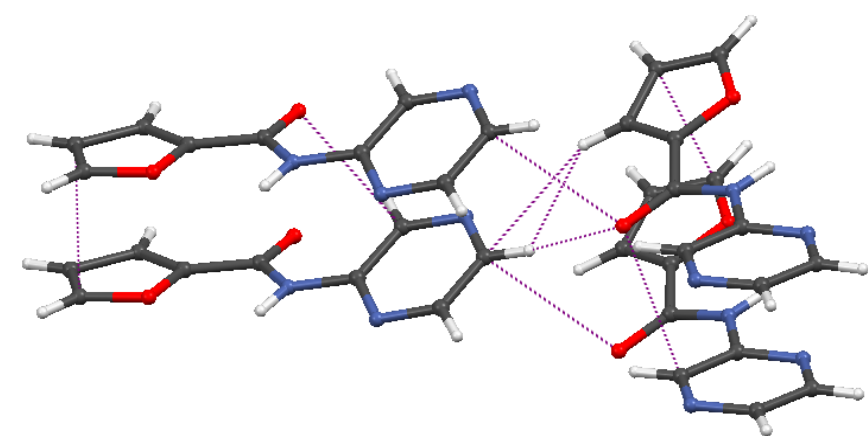
Tet 11



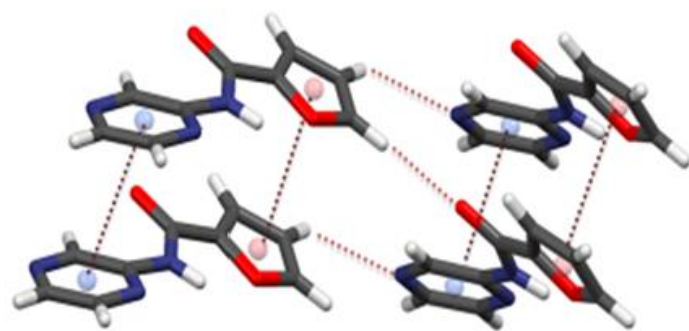
Tet 12



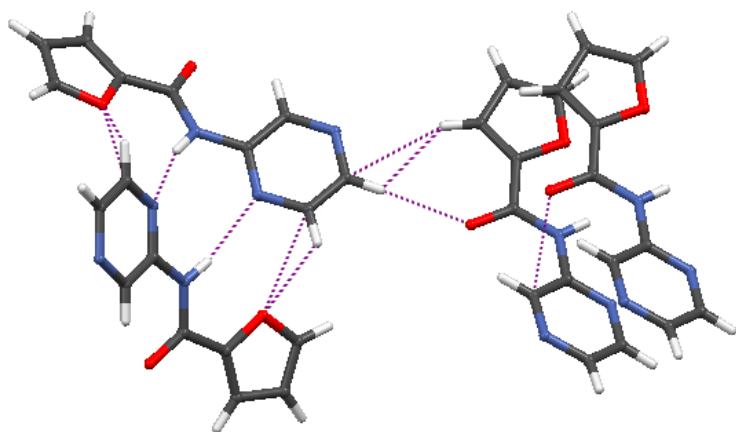
Tet 13



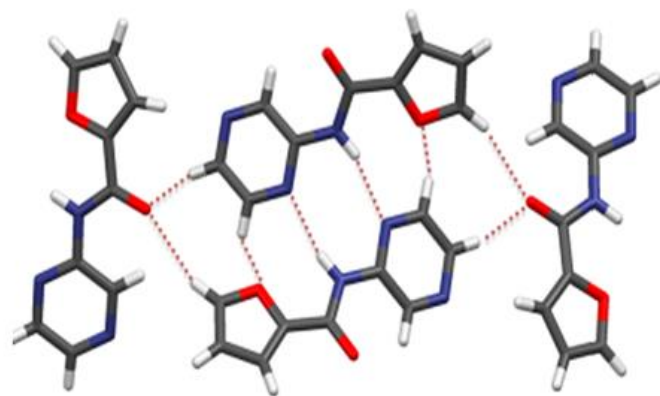
Tet 14



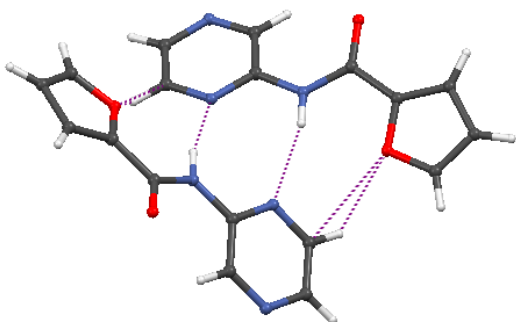
Tet 15



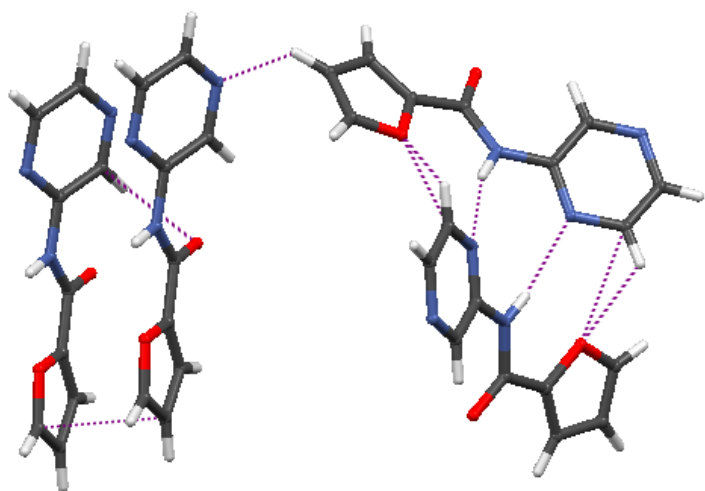
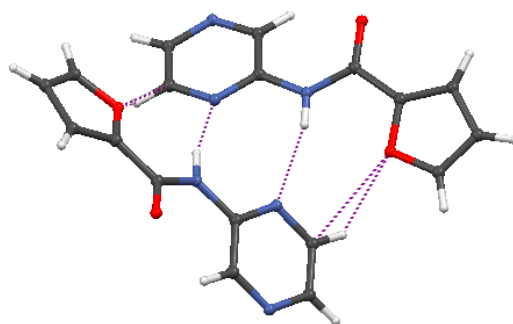
Tet 16



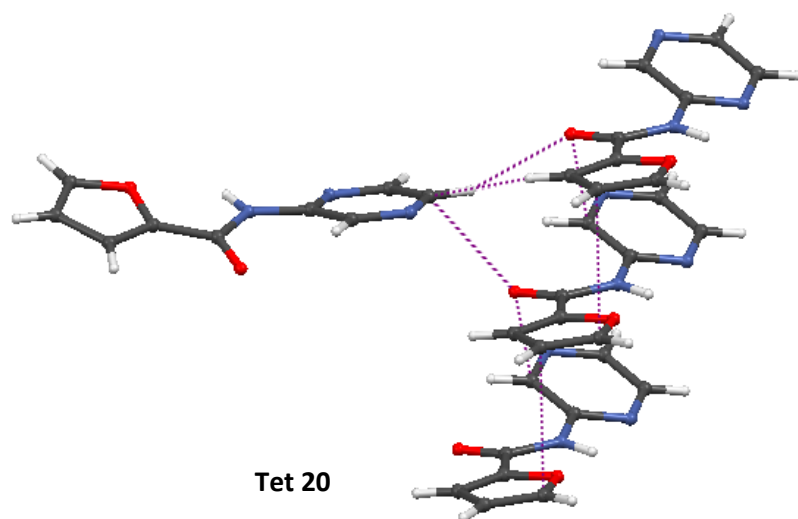
Tet 17



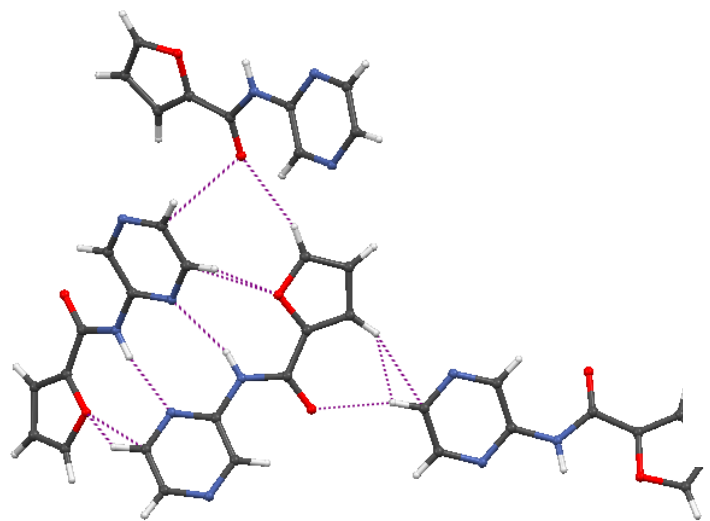
Tet 18



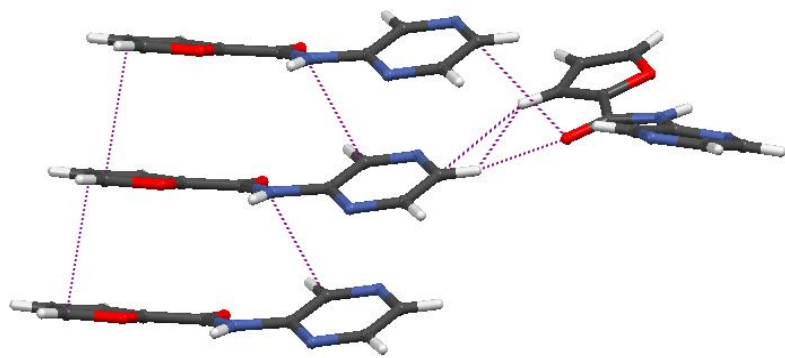
Tet 19



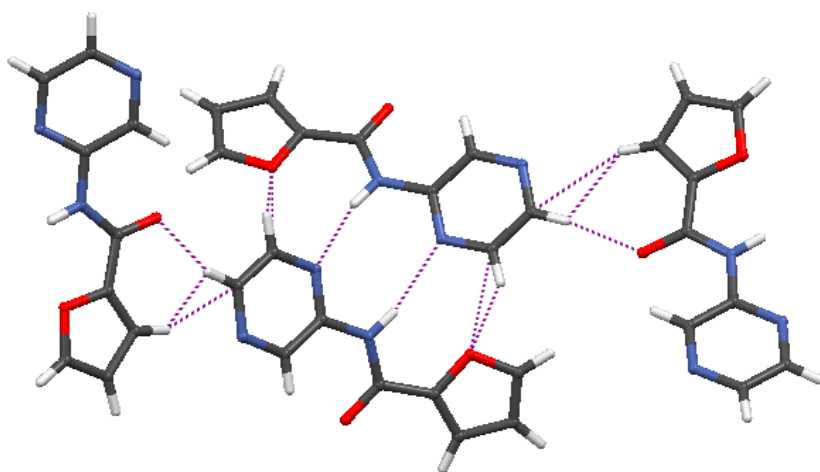
Tet 20



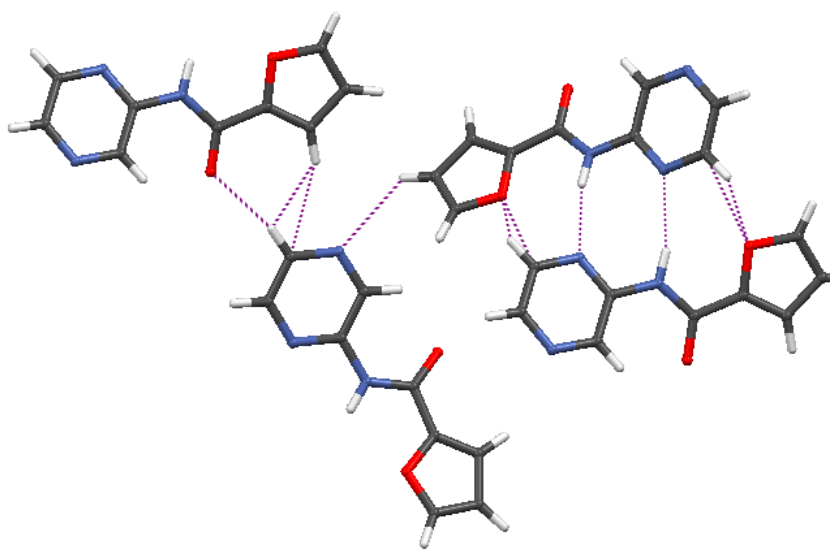
Tet 21



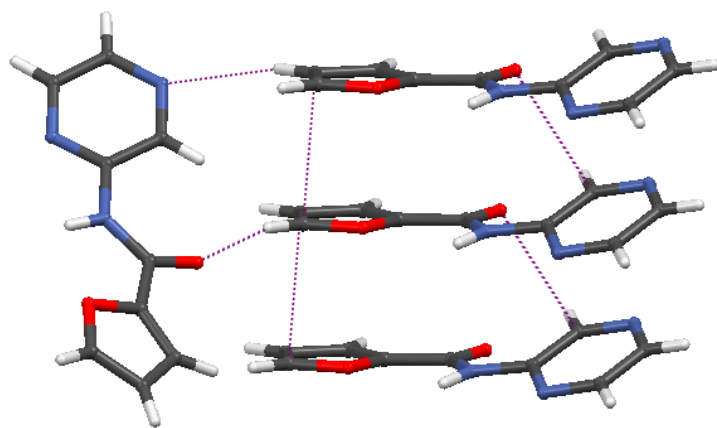
Tet 22



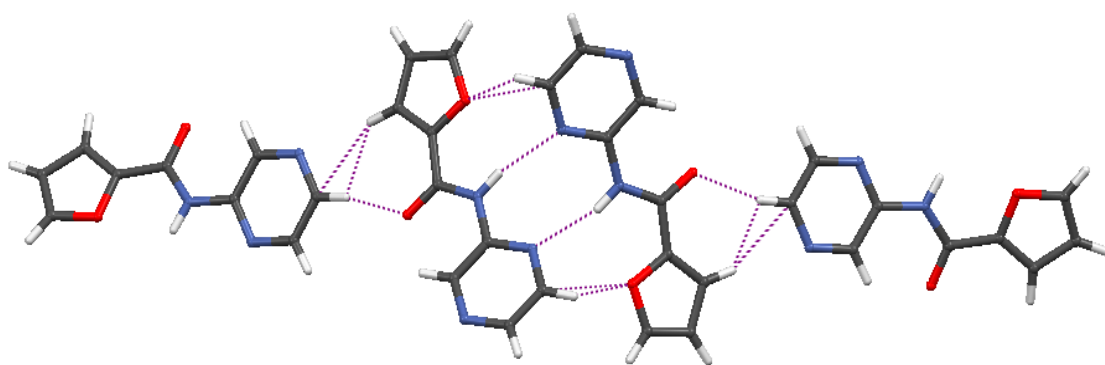
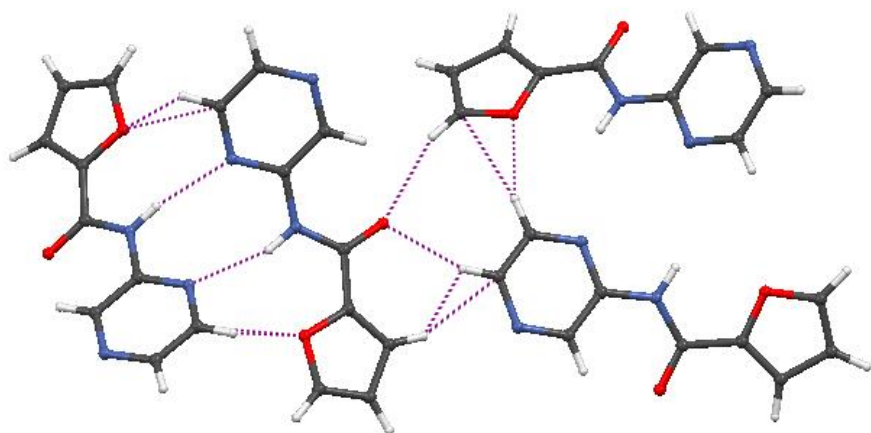
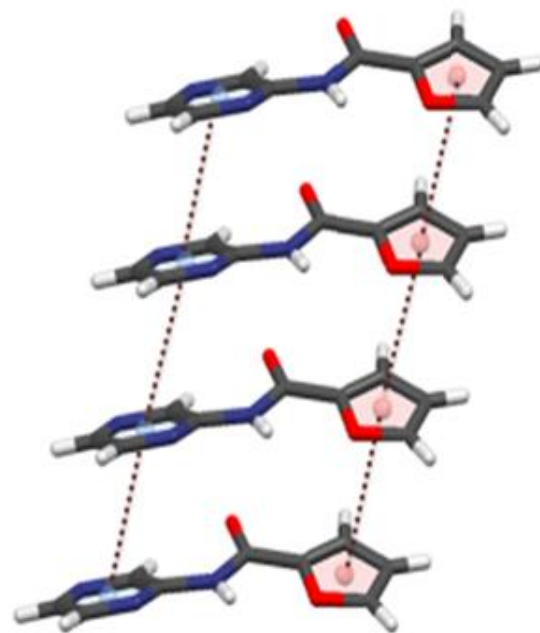
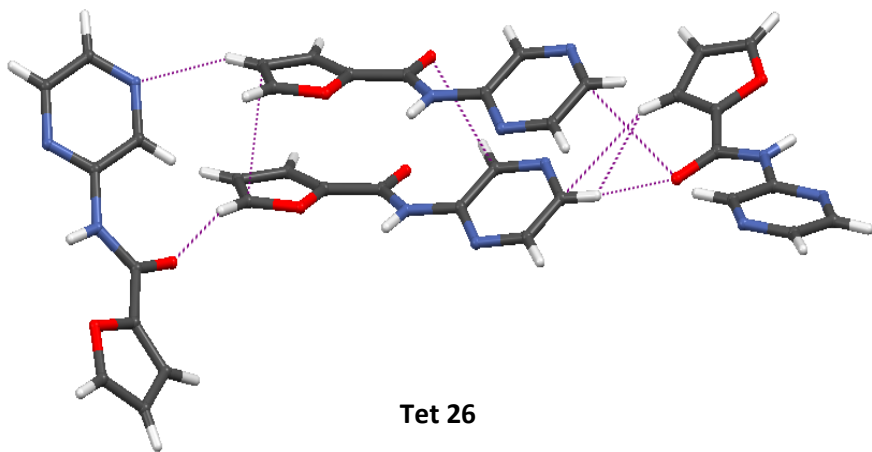
Tet 23

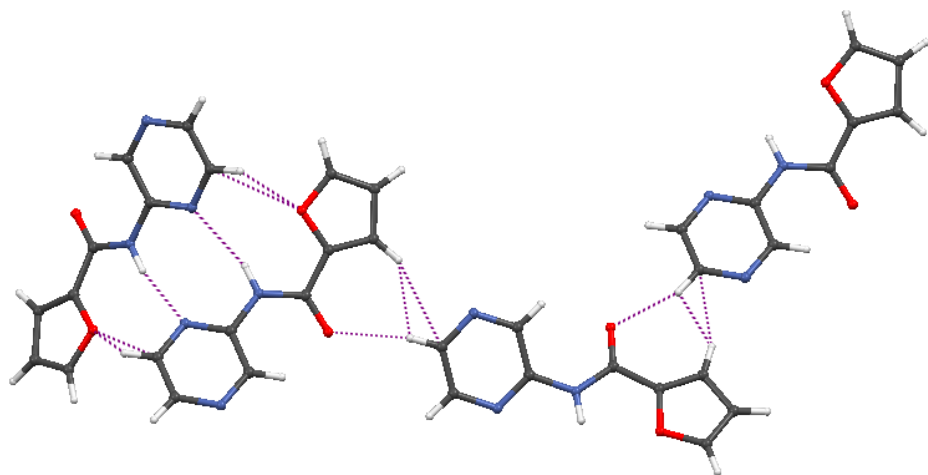


Tet 24

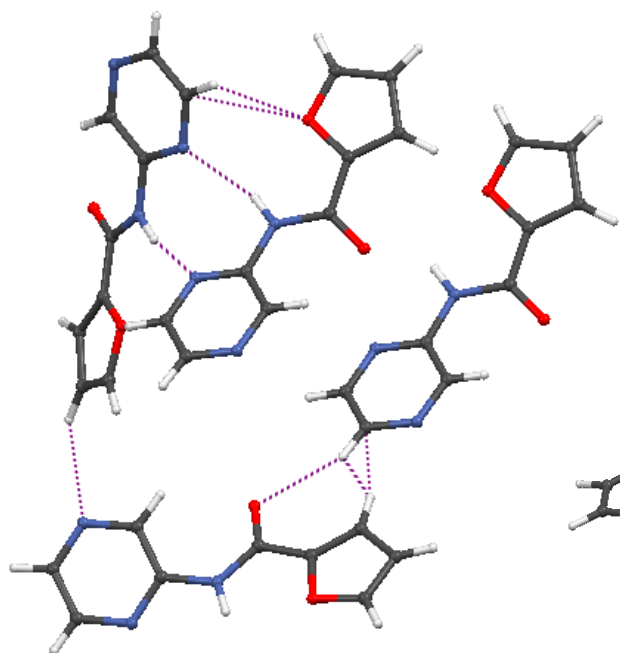


Tet 25

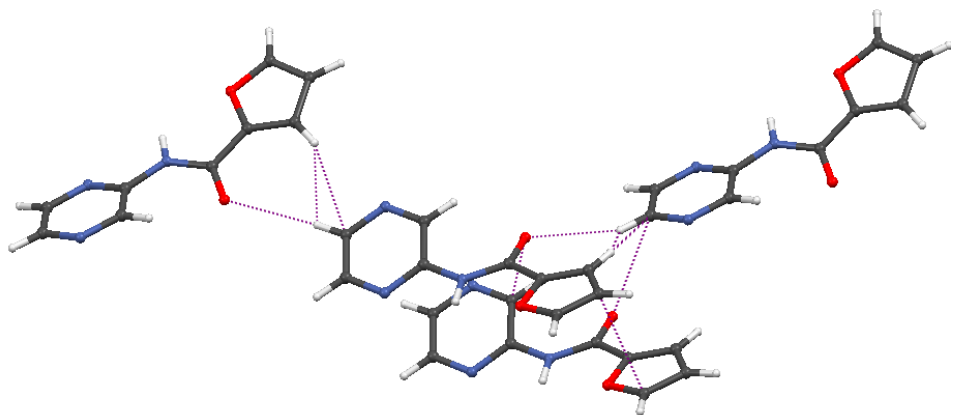




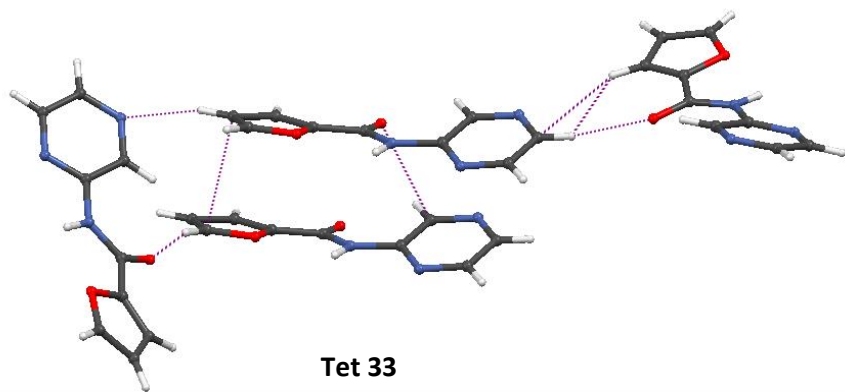
Tet 30



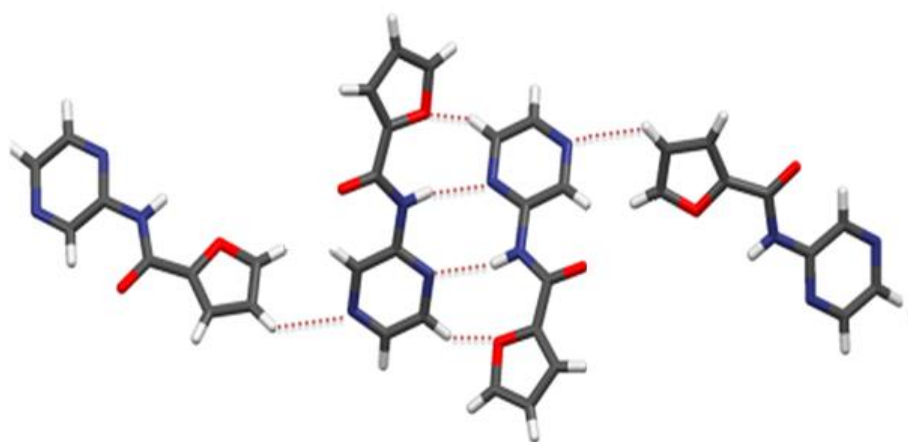
Tet 31



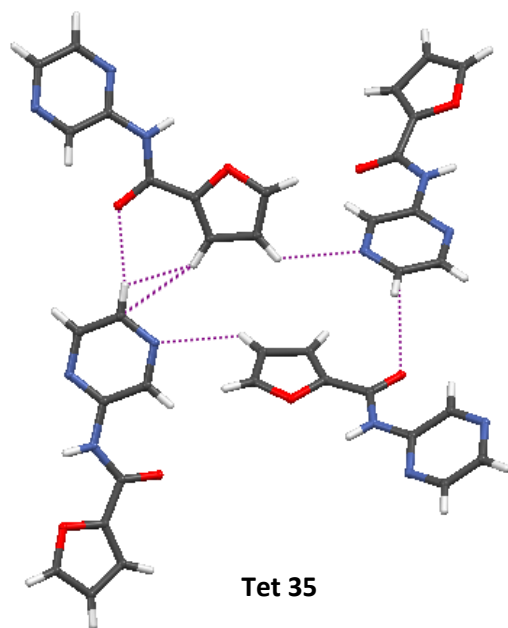
Tet 32



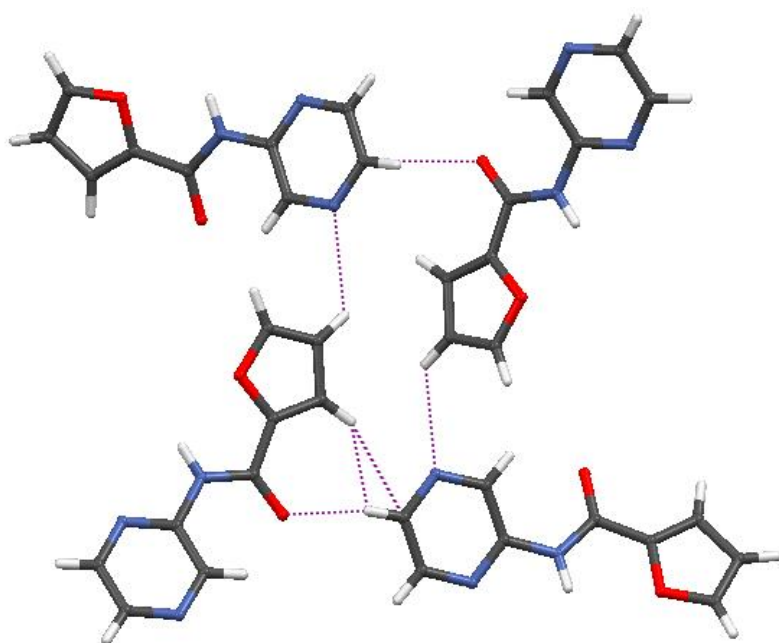
Tet 33



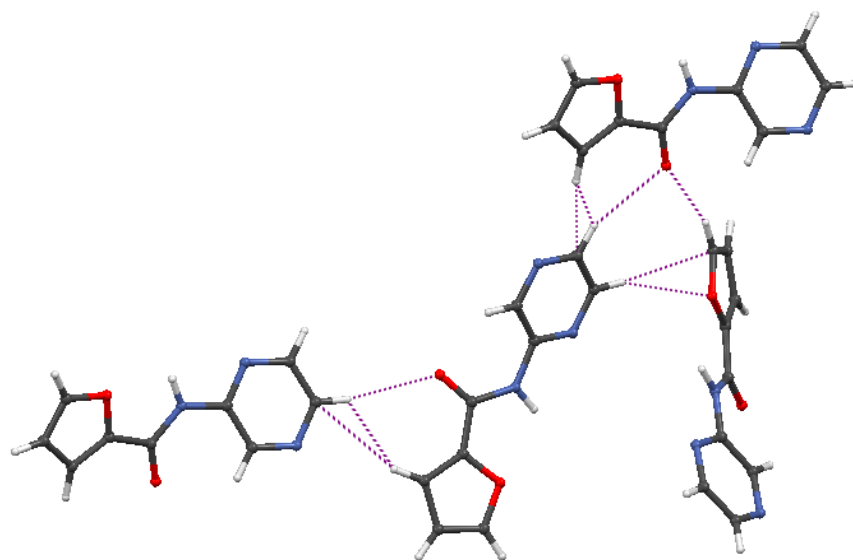
Tet 34



Tet 35

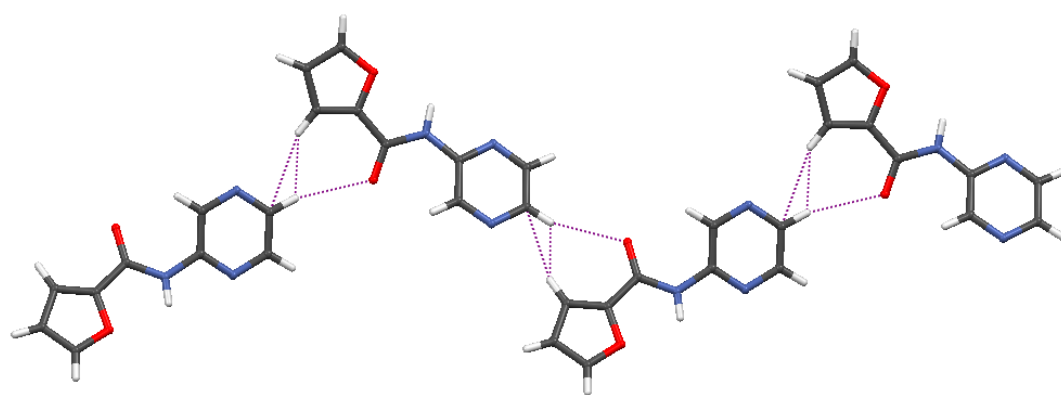


Tet 36

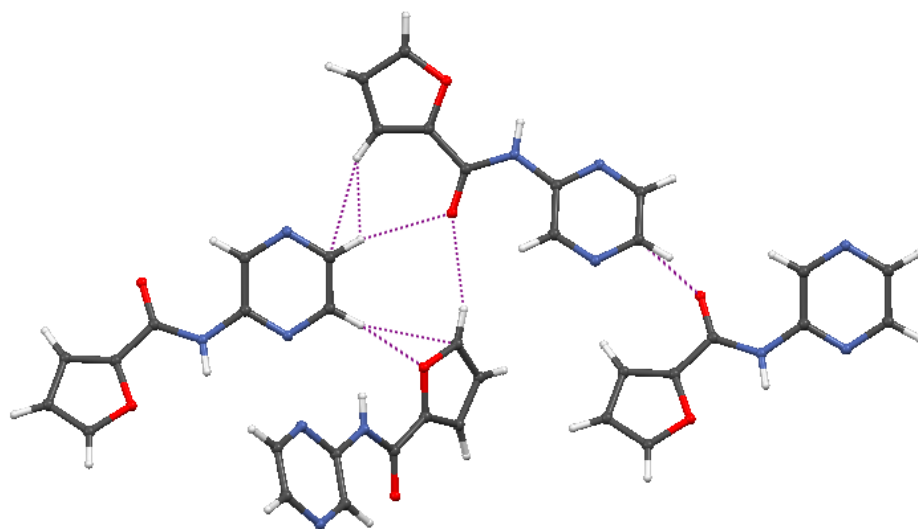


S32

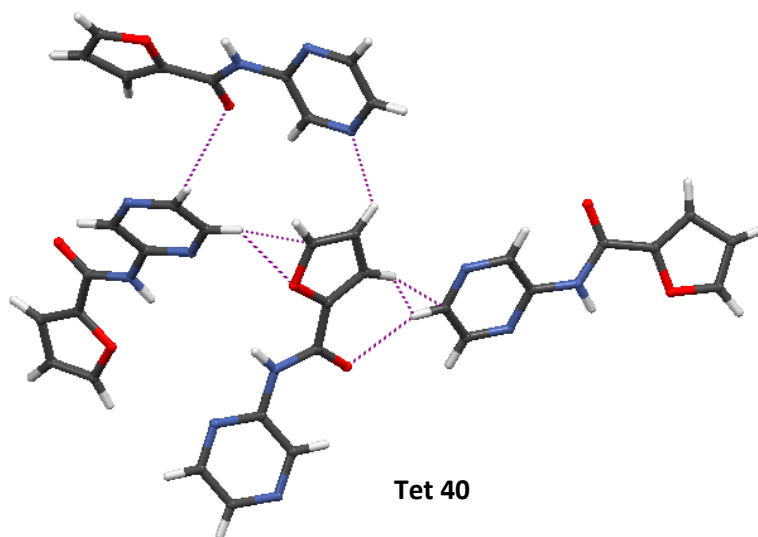
Tet 37



Tet 38

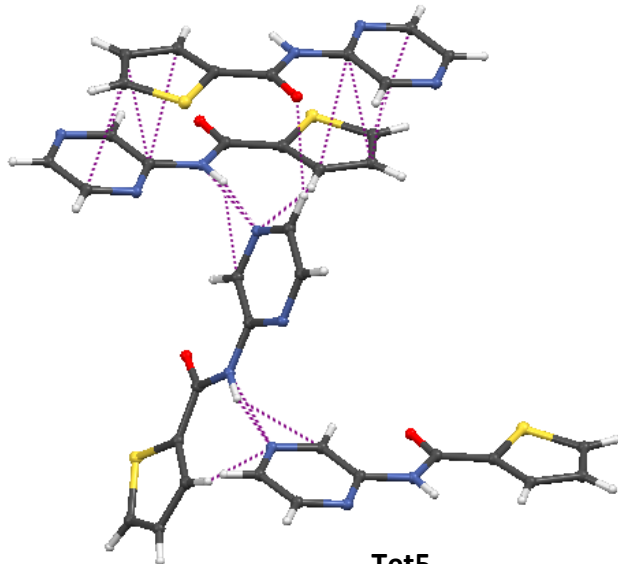
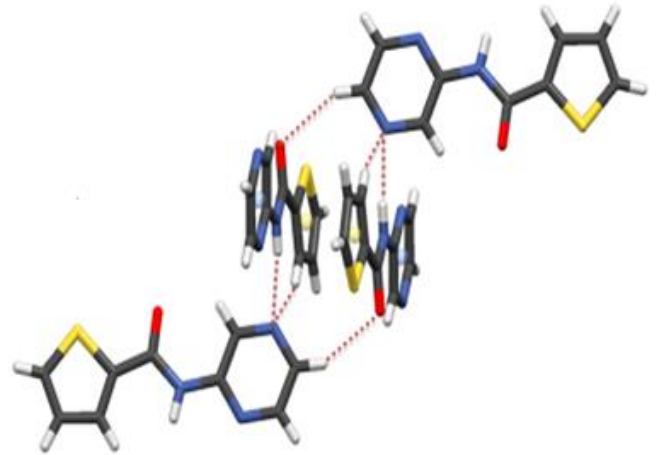
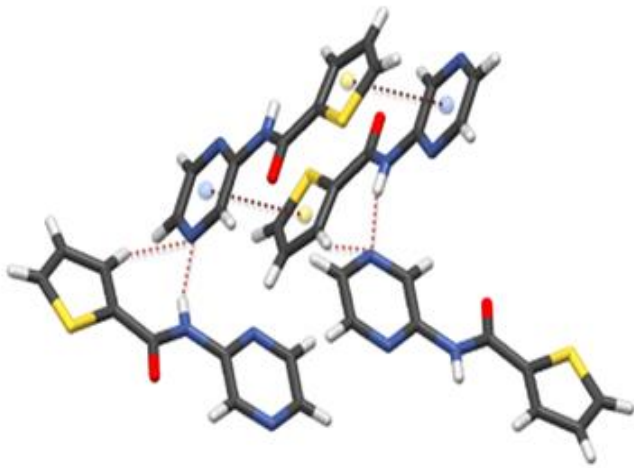
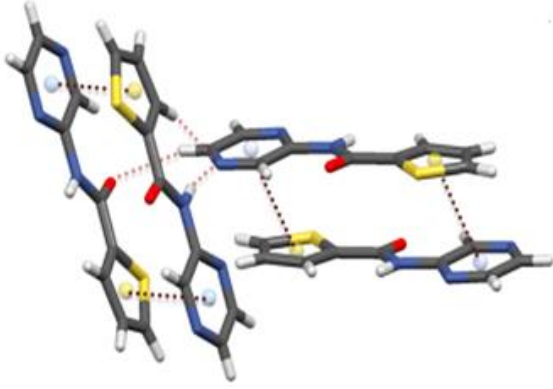


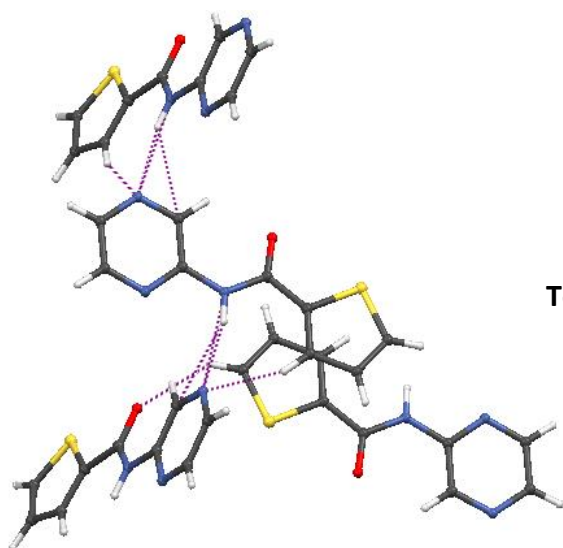
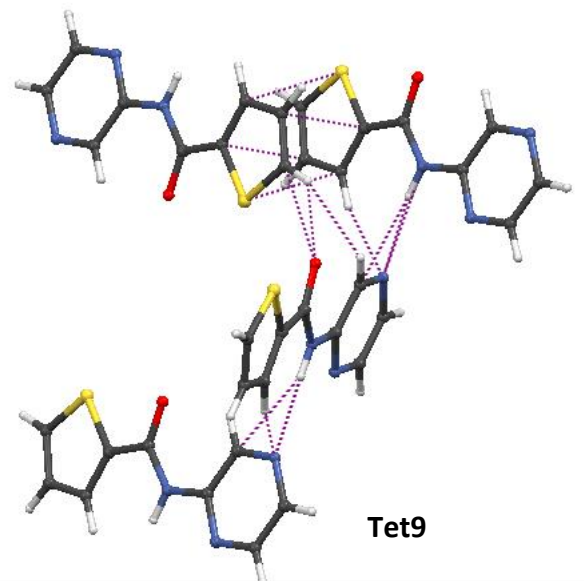
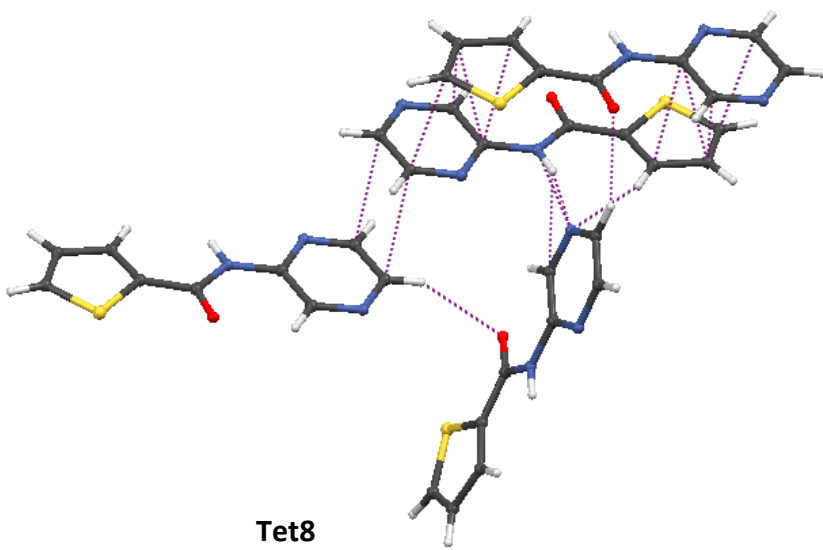
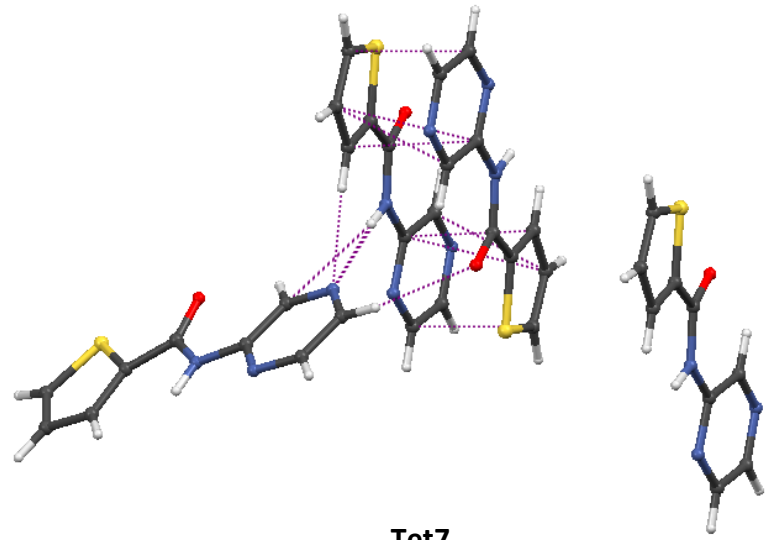
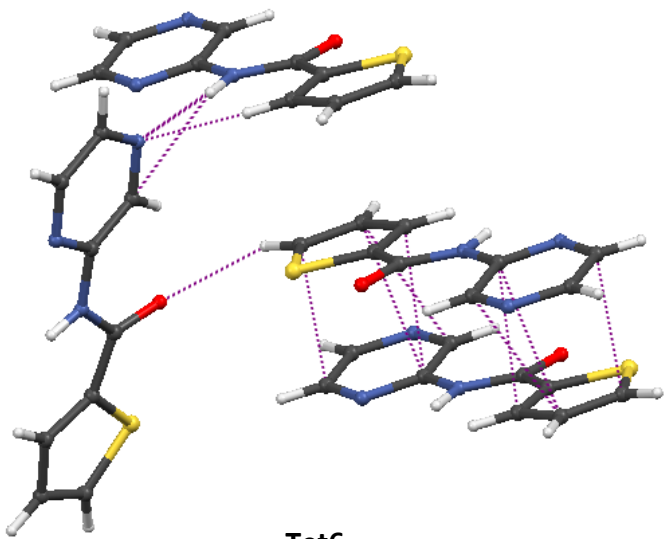
Tet 39

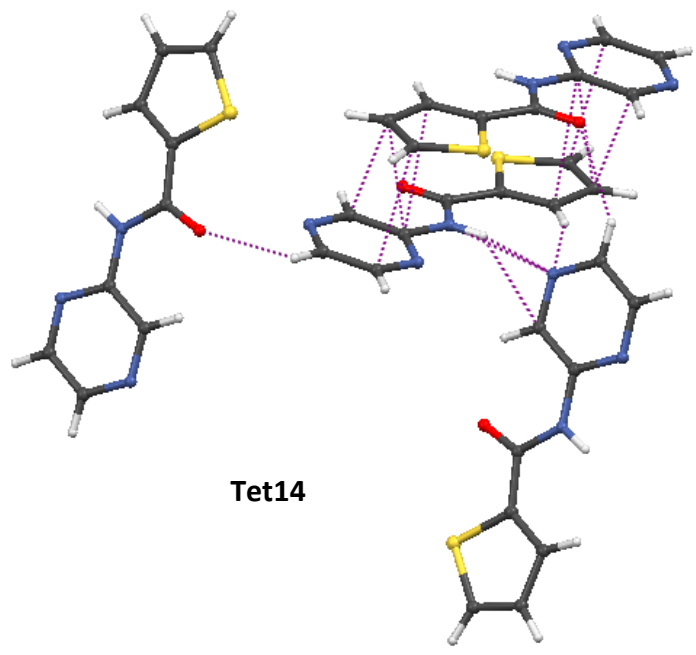
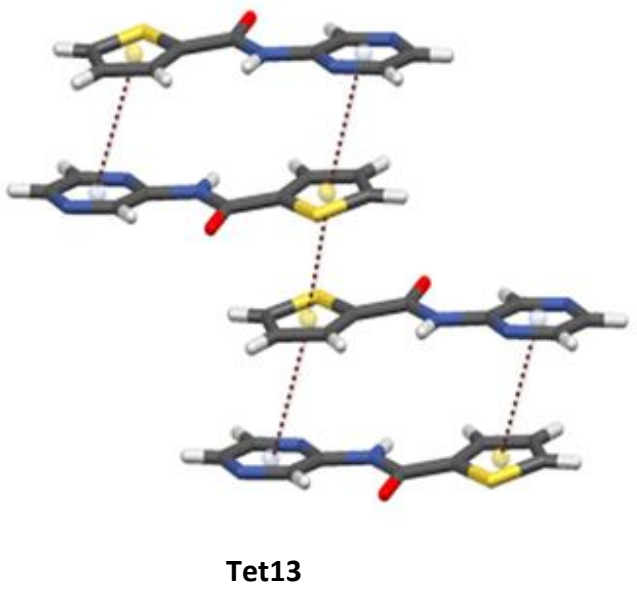
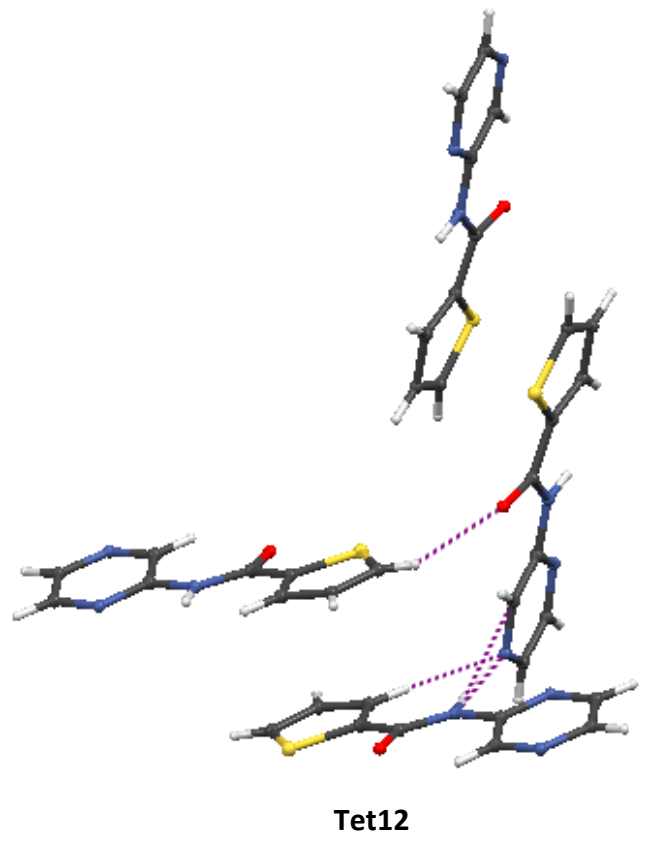
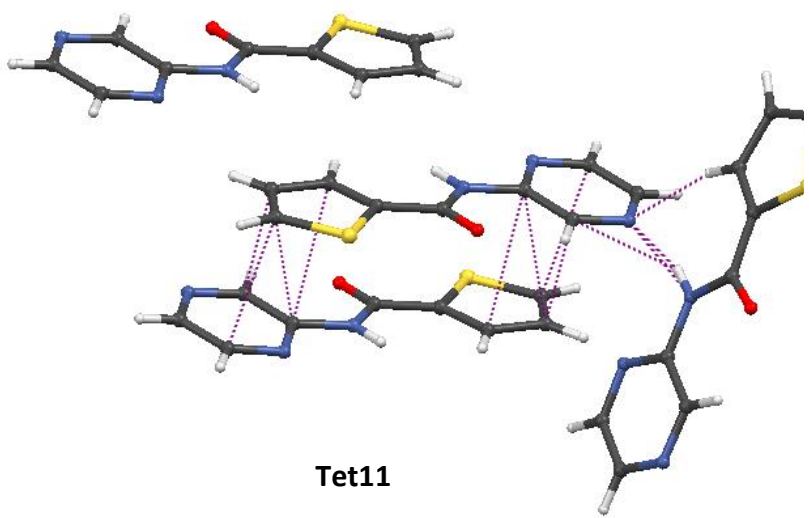


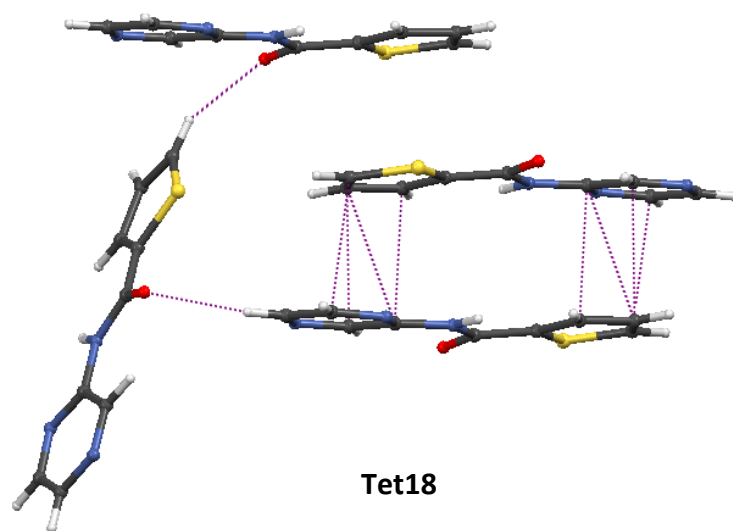
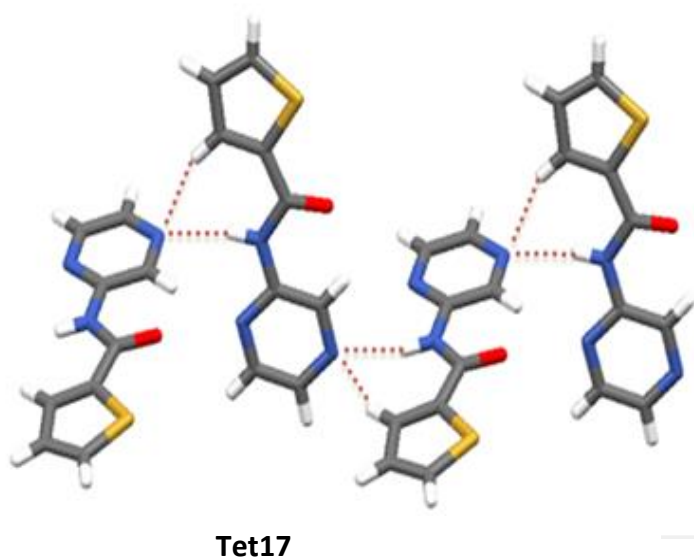
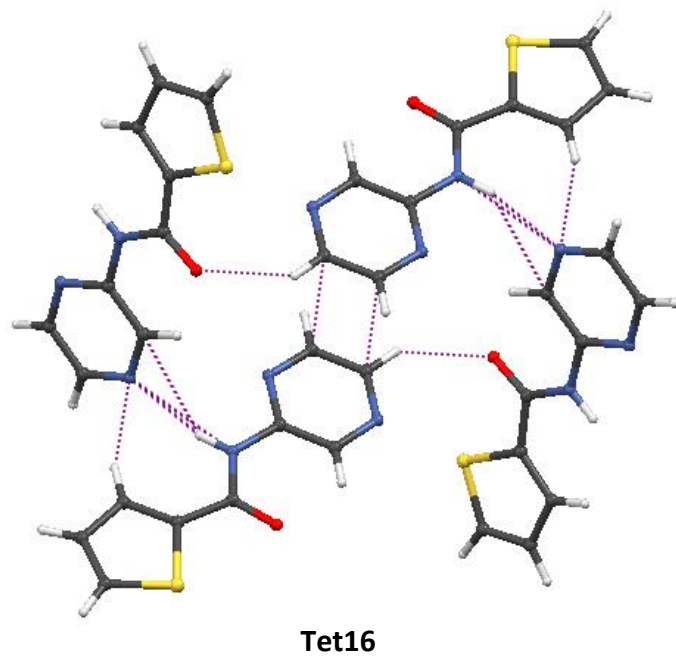
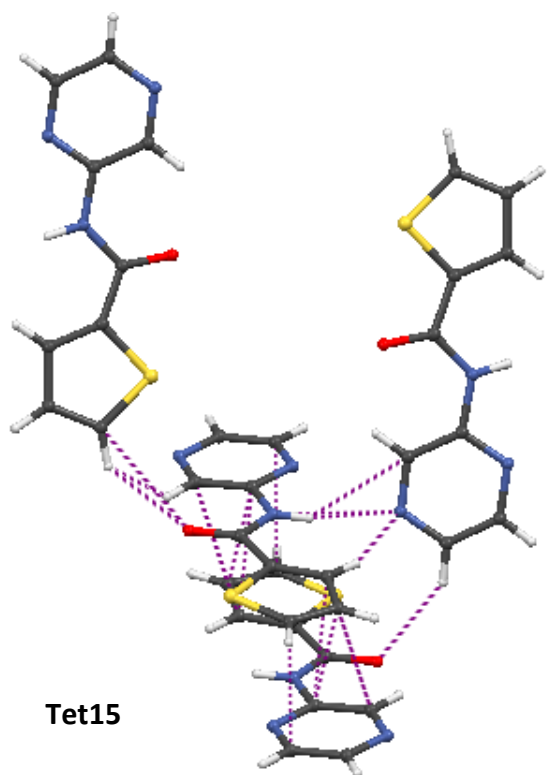
Tet 40

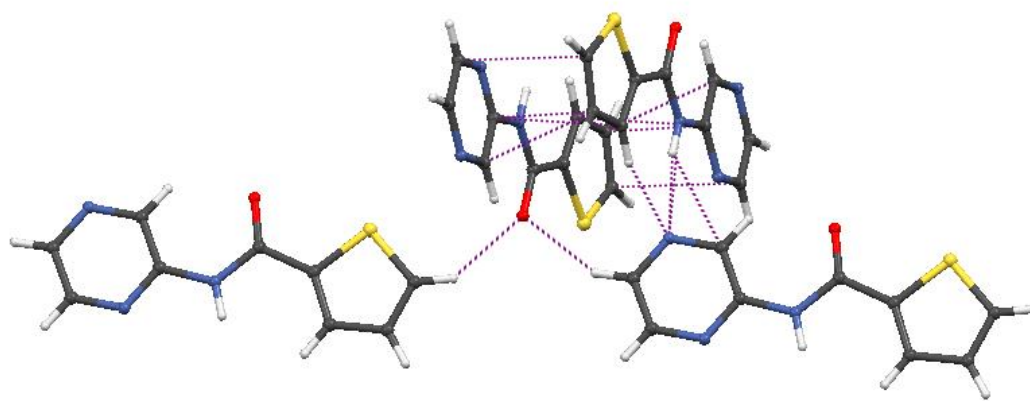
Figure S22. Representation of the most stable tetramer motifs of I which are labeled based on the interaction energy ranking



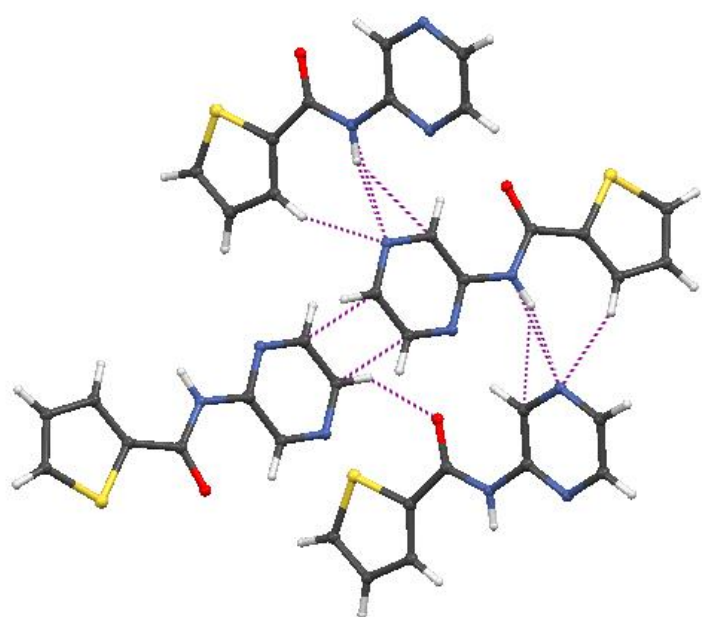




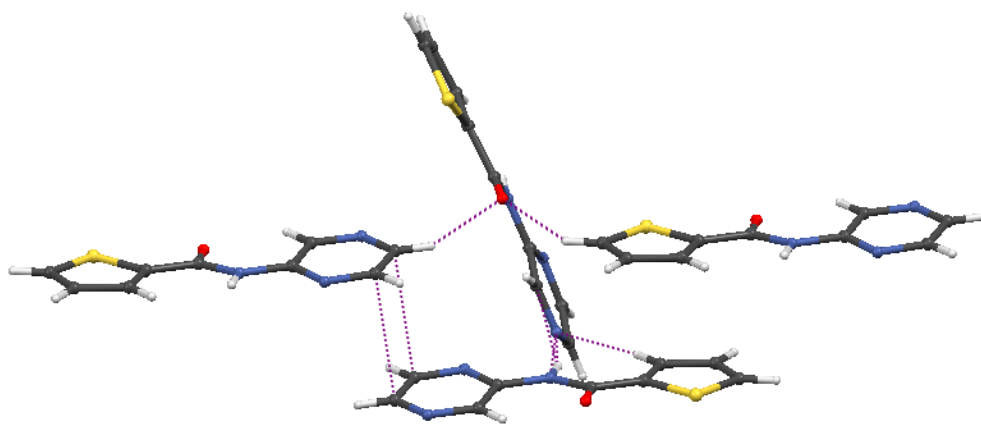




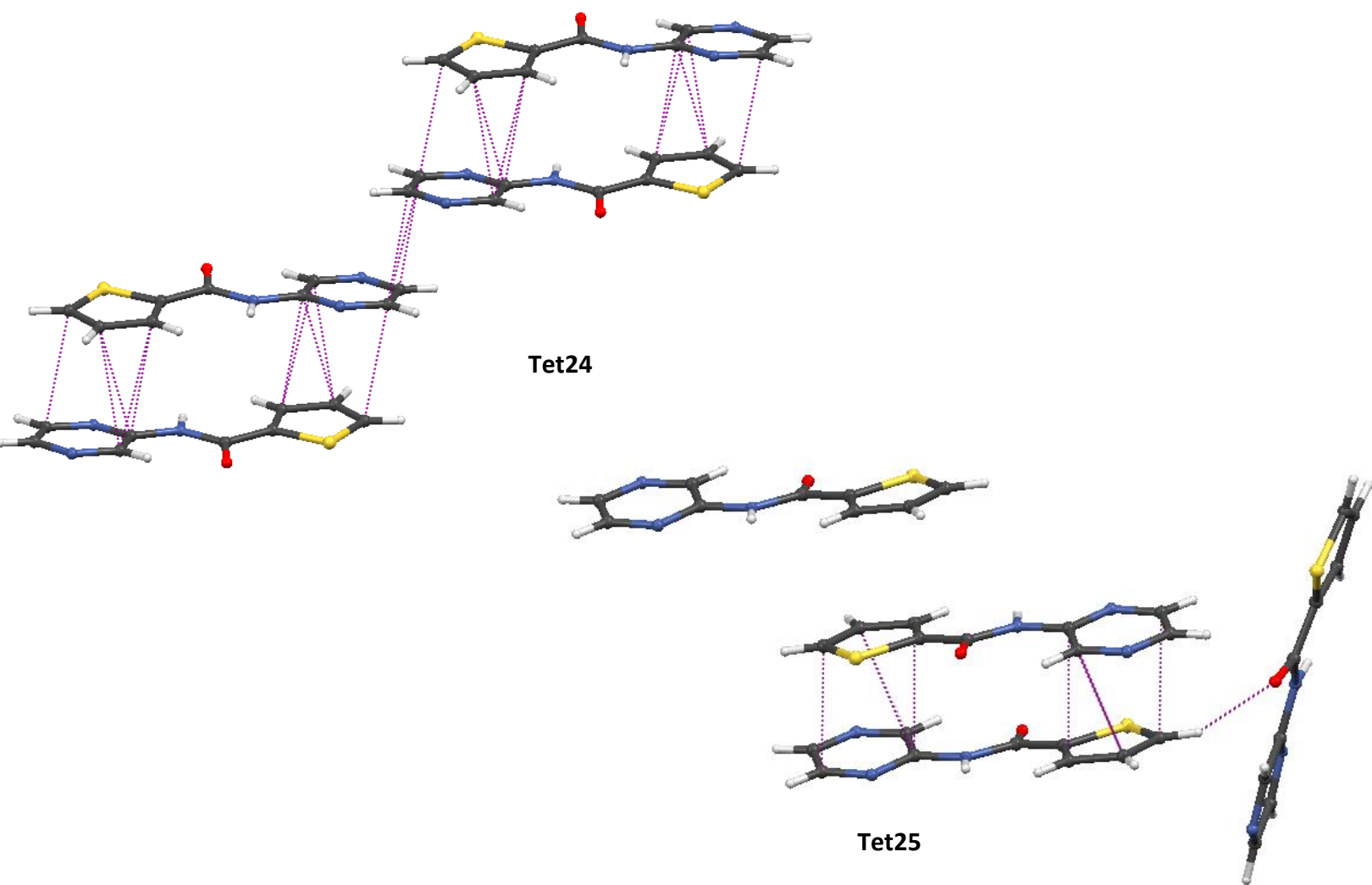
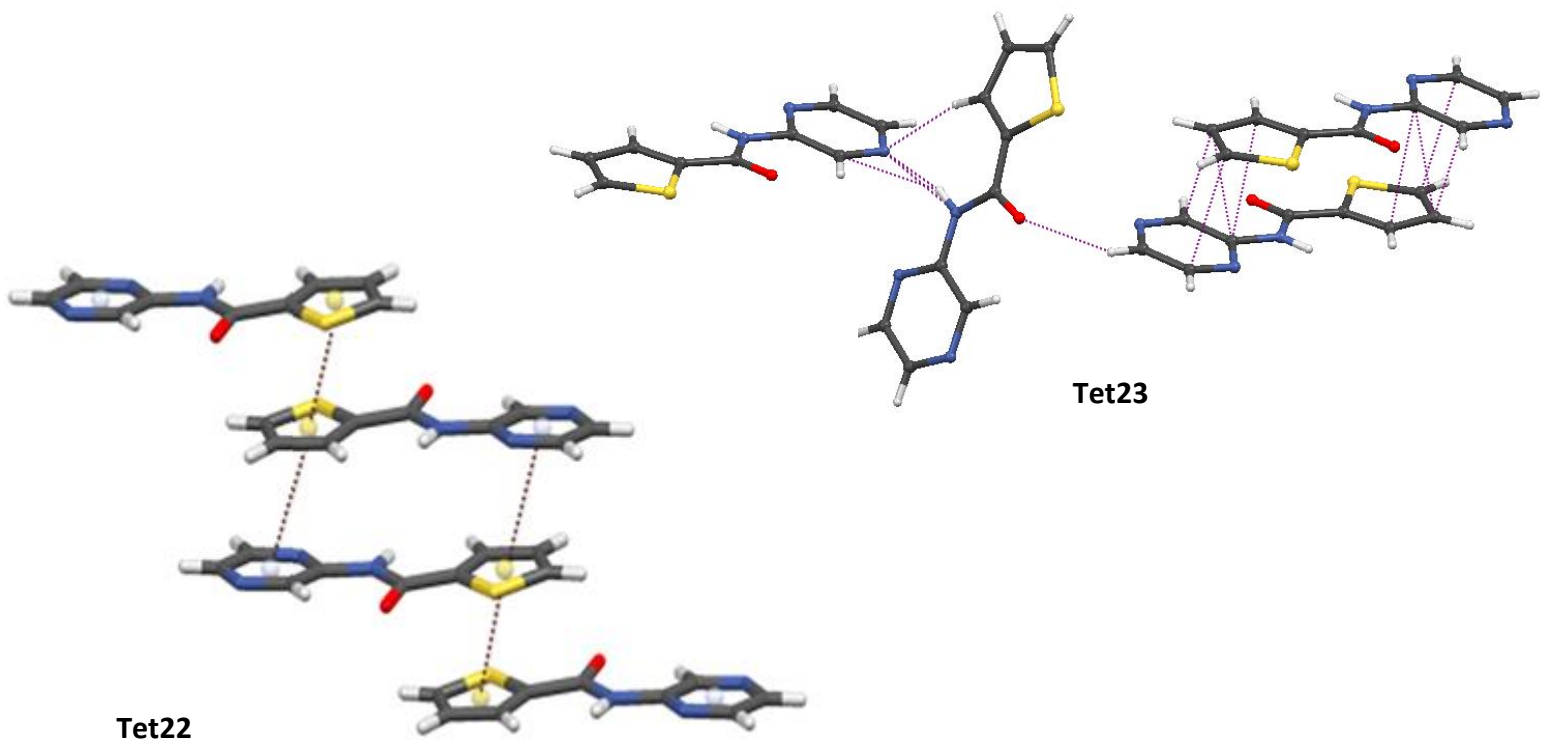
Tet19

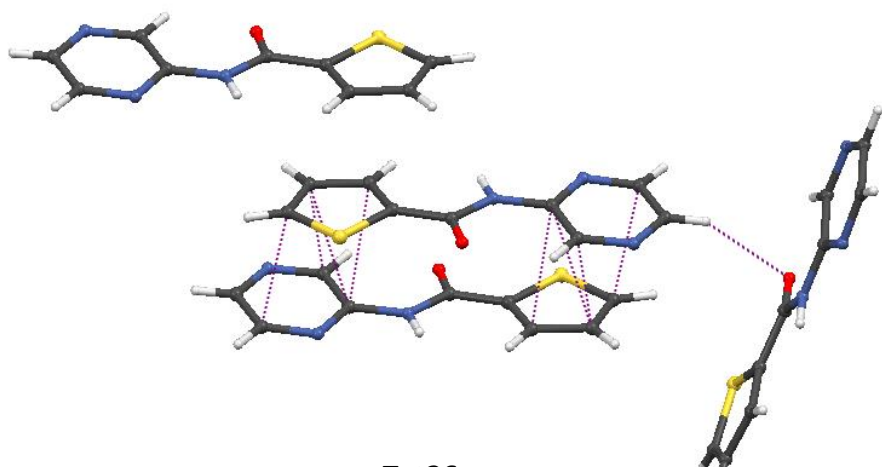


Tet20

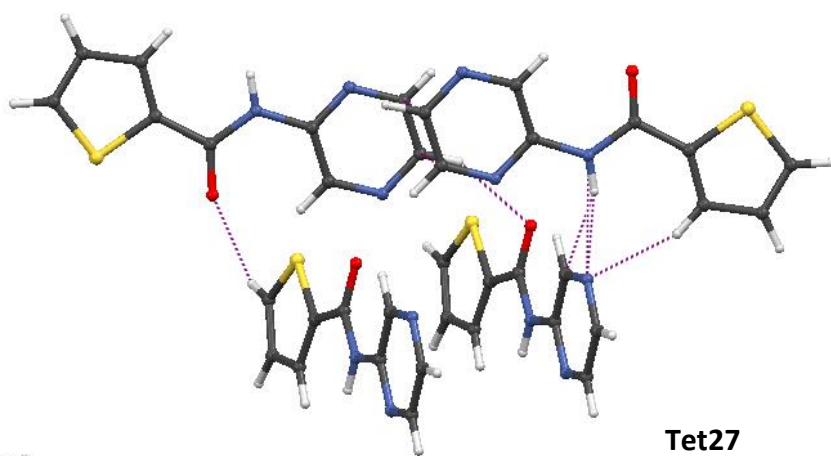


Tet21

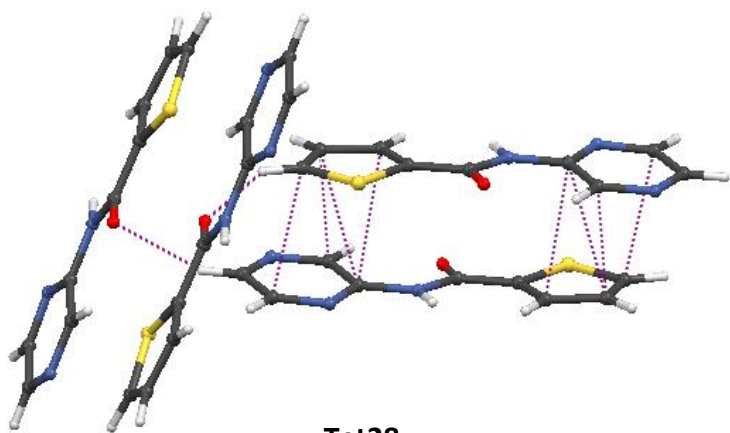




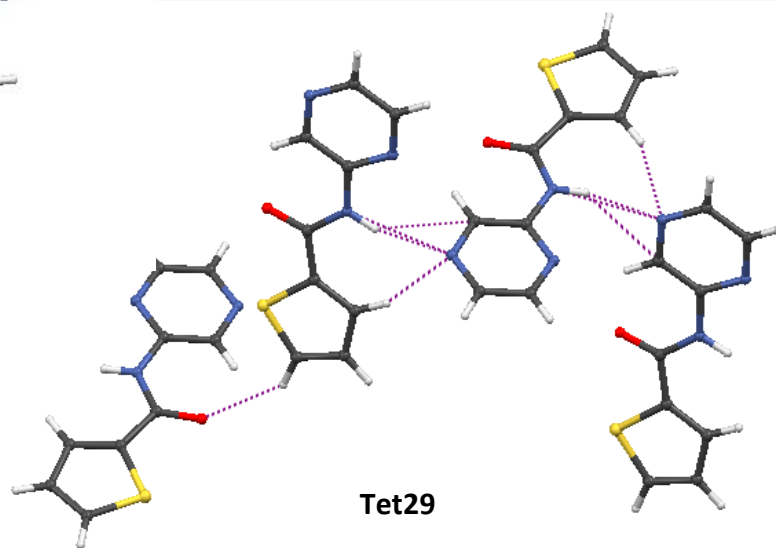
Tet26



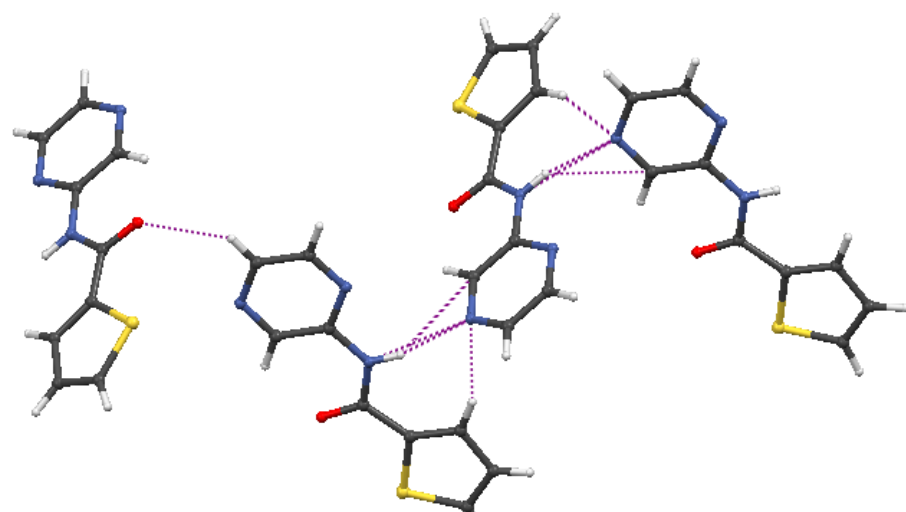
Tet27



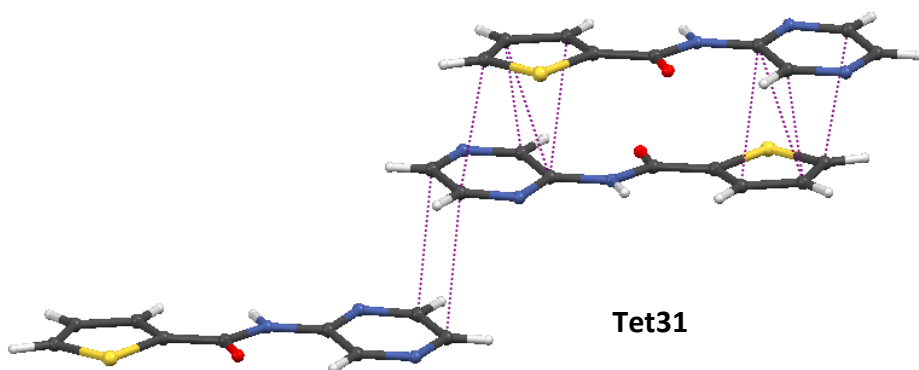
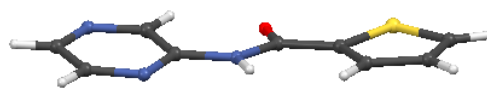
Tet28



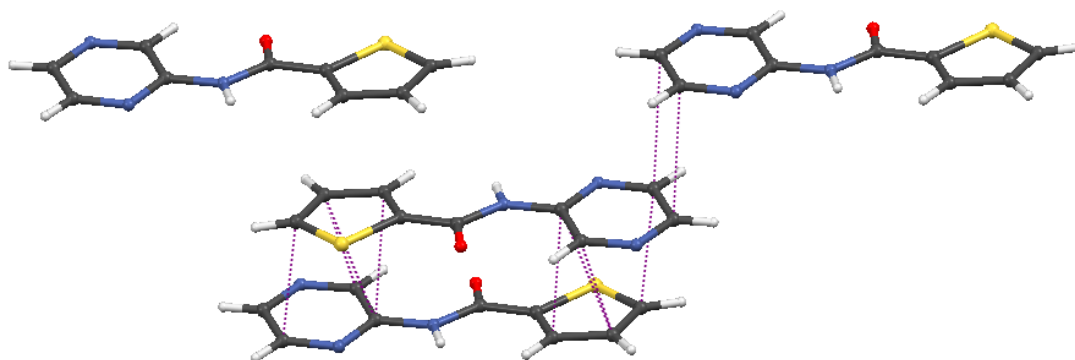
Tet29



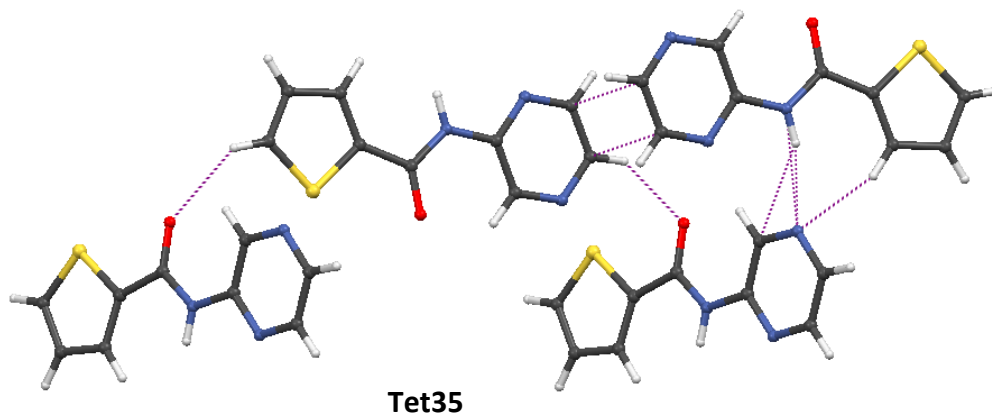
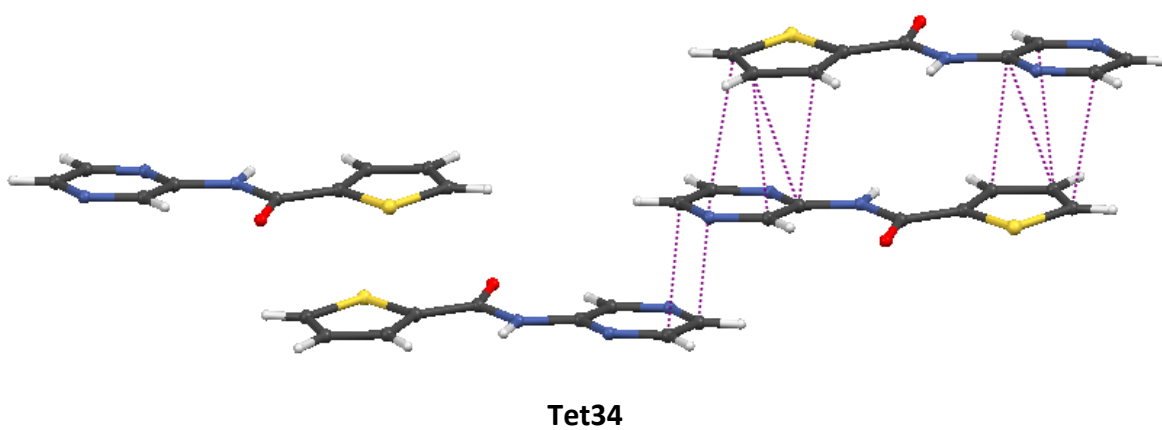
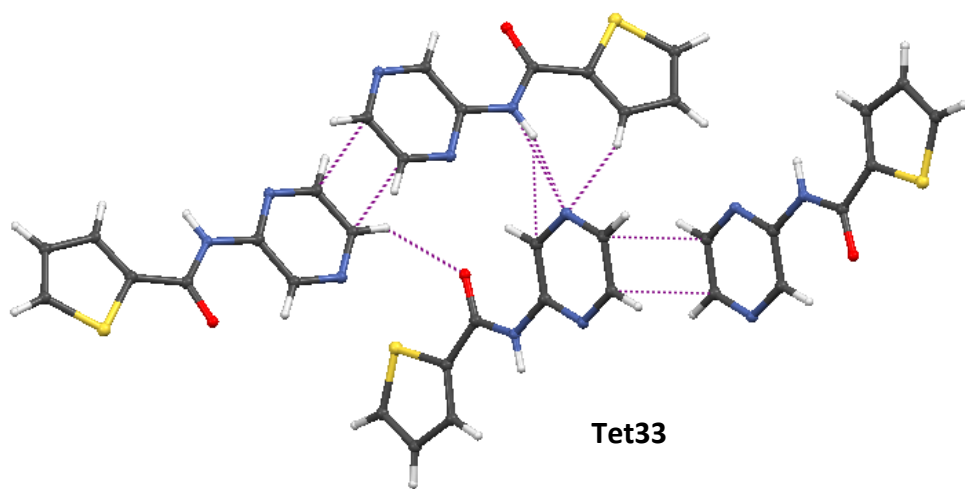
Tet30

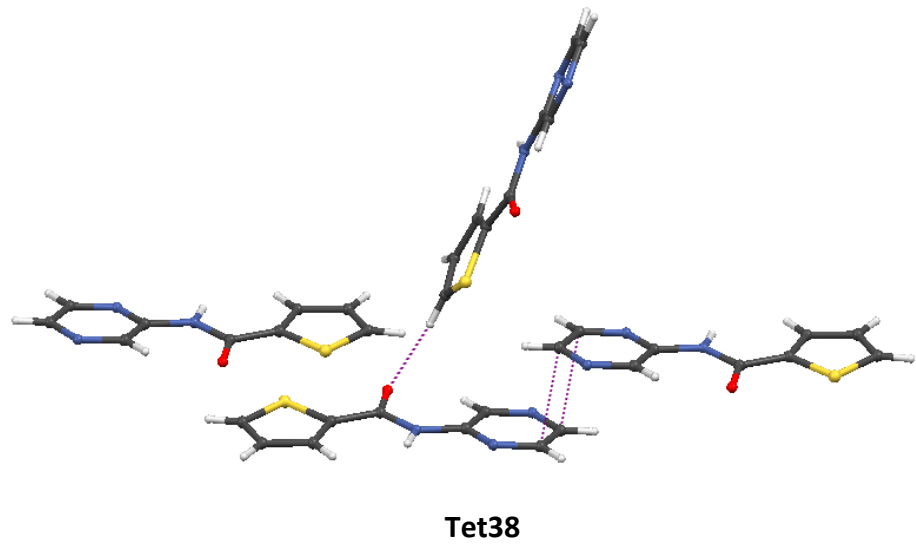
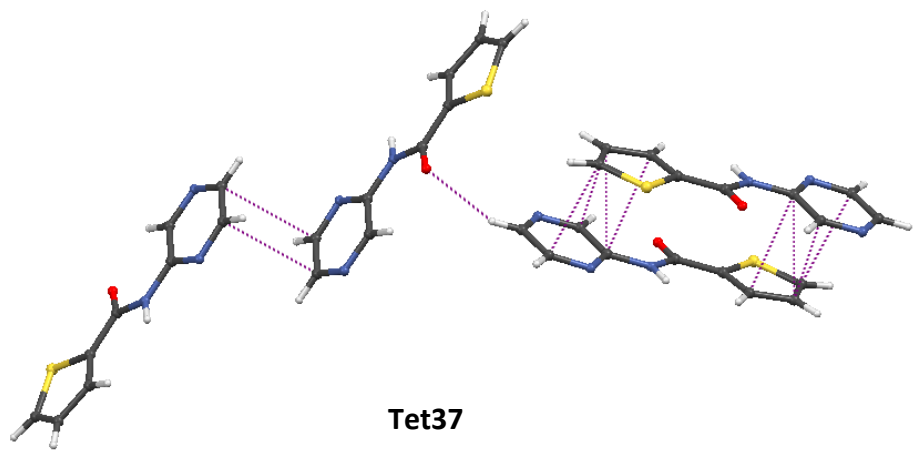
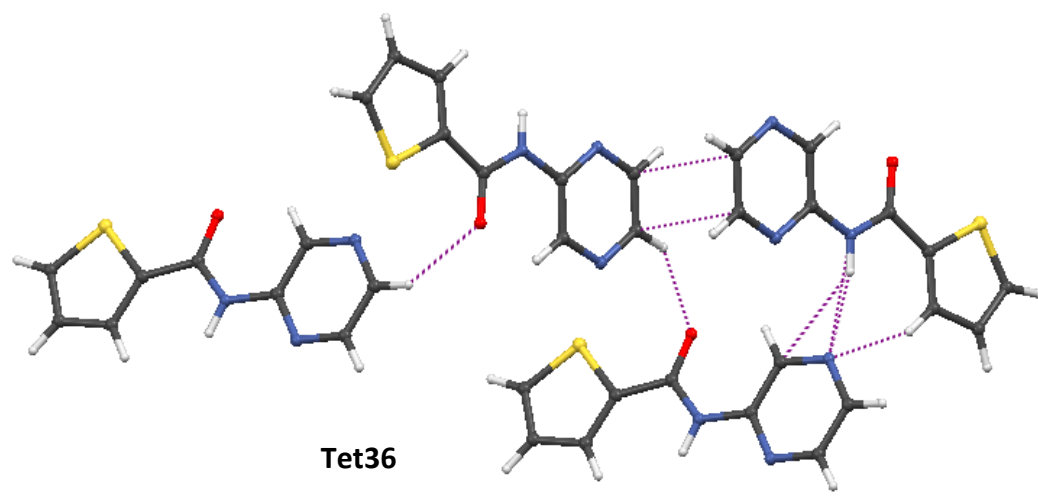


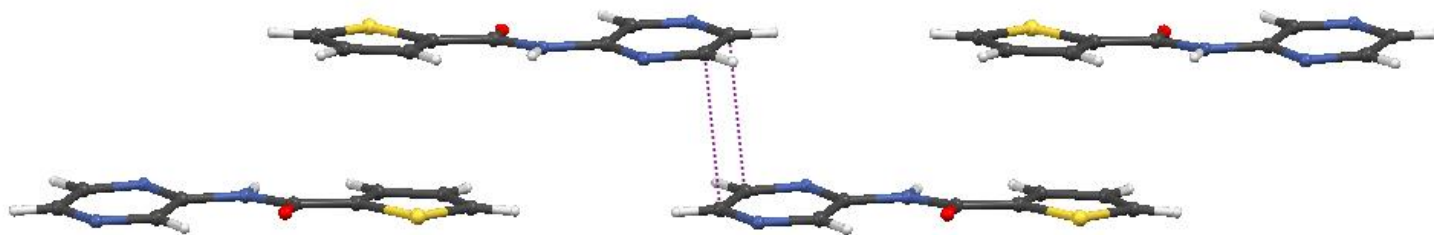
Tet31



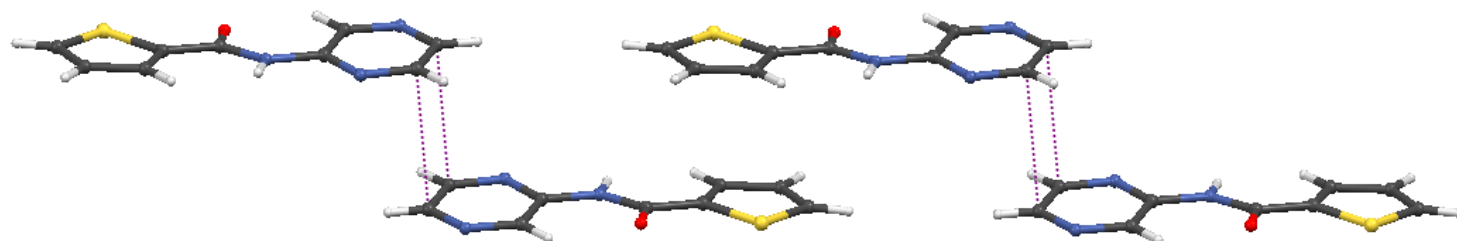
Tet32







Tet39



Tet40

Figure S23. Representation of the most stable tetramer motifs of *II* which are labeled based on the interaction energy ranking

Table S1. The binding energy (E_{calc} in kJ/mol) of the most stable tetramer fragments of compound *I*, along with contribution of cooperativity (E_{coop}), HB (E_{HB}) and $\pi\cdots\pi$ stacking ($E_{\pi\cdots\pi}$) energies as the magnitude (in kJ/mol) and percentage of total binding energy, as well as their weighted contributions.

| Furan | | E_{Calc} | E_{coop} | % E_{coop} | %W E_{coop} | E_{HB} | %HB | %W HB | E π -based | % π -based | %W π -based |
|------------|---|-------------------|-------------------|------------------------|-------------------------|-----------------|--------|--------------|-------------------|-------------------|--------------------|
| Tet1 | 2D1 (HB)+2D2 ($\pi\cdots\pi$)+2D7 (HB) | -160.27 | -1.18 | 0.74 | 0.03 | -103.01 | 64.27 | 2.78 | -56.08 | 34.99 | 1.52 |
| Tet2 | D1 (HB)+D2 ($\pi\cdots\pi$)+D3 (HB)+D6 (HB)+D4 (HB) | -119.22 | -1.95 | 1.64 | 0.05 | -89.23 | 74.85 | 2.41 | -28.04 | 23.52 | 0.76 |
| Tet3 | D1 (HB)+D2 ($\pi\cdots\pi$)+D5 (HB)+D6 (HB)+D4 (HB)+D7 (HB) | -118.97 | -0.51 | 0.43 | 0.01 | -90.42 | 76.00 | 2.44 | -28.04 | 23.57 | 0.76 |
| Tet4 | D1 (HB)+2D2 ($\pi\cdots\pi$)+2D7 (HB) | -116.75 | -1.85 | 1.59 | 0.05 | -58.82 | 50.38 | 1.59 | -56.08 | 48.03 | 1.52 |
| Tet5 | D1 (HB)+2D2 ($\pi\cdots\pi$)+2D7 (HB) | -116.38 | -1.48 | 1.28 | 0.04 | -58.82 | 50.54 | 1.59 | -56.08 | 48.19 | 1.52 |
| Tet6 | 2D1 (HB)+D6 (HB)+D4 (HB) | -113.71 | -0.16 | 0.14 | 0.00 | -113.55 | 99.86 | 3.07 | 0.00 | 0.00 | 0.00 |
| Tet7 | D1 (HB)+D2 ($\pi\cdots\pi$)+D3 (HB)+D6 (HB)+D7 (HB) | -112.72 | 0.77 | -0.68 | -0.02 | -85.45 | 75.81 | 2.31 | -28.04 | 24.87 | 0.76 |
| Tet8 | D1 (HB)+D2 ($\pi\cdots\pi$)+D5 (HB)+D6 (HB)+D4 (HB) | -112.48 | -1.33 | 1.18 | 0.04 | -83.11 | 73.89 | 2.25 | -28.04 | 24.93 | 0.76 |
| Tet9 | D1 (HB)+D2 ($\pi\cdots\pi$)+D3 (HB)+D6 (HB)+D7 (HB) | -111.13 | -0.30 | 0.27 | 0.01 | -82.79 | 74.50 | 2.24 | -28.04 | 25.23 | 0.76 |
| Tet10 | 2D1 (HB)+D3 (HB) | -110.44 | -2.17 | 1.96 | 0.06 | -108.27 | 98.04 | 2.93 | 0.00 | 0.00 | 0.00 |
| Tet11 | D1 (HB)+2D2 ($\pi\cdots\pi$)+D7 (HB) | -109.38 | -1.79 | 1.64 | 0.05 | -51.51 | 47.09 | 1.39 | -56.08 | 51.27 | 1.52 |
| Tet12 | 2D1 (HB)+D5 (HB) | -104.59 | -2.45 | 2.34 | 0.07 | -102.15 | 97.66 | 2.76 | 0.00 | 0.00 | 0.00 |
| Tet13 | D1 (HB)+D2 ($\pi\cdots\pi$)+D3 (HB)+D6 (HB) | -103.14 | 0.38 | -0.37 | -0.01 | -75.48 | 73.18 | 2.04 | -28.04 | 27.19 | 0.76 |
| Tet14 | 2D2 ($\pi\cdots\pi$)+D3 (HB)+2D6 (HB) | -99.74 | -0.98 | 0.98 | 0.03 | -42.68 | 42.80 | 1.15 | -56.08 | 56.22 | 1.52 |
| Tet15 | 2D2 ($\pi\cdots\pi$)+2D5 (HB)+D4 (HB) | -96.35 | 0.99 | -1.03 | -0.03 | -41.26 | 42.83 | 1.12 | -56.08 | 58.20 | 1.52 |
| Tet16 | D1 (HB)+D2 ($\pi\cdots\pi$)+D3 (HB) | -96.03 | -3.92 | 4.08 | 0.11 | -64.08 | 66.72 | 1.73 | -28.04 | 29.20 | 0.76 |
| Tet17 | D1 (HB)+2D6 (HB)+2D4 (HB) | -94.74 | -0.23 | 0.24 | 0.01 | -94.51 | 99.76 | 2.56 | 0.00 | 0.00 | 0.00 |
| Tet18 | 2D1 (HB)+D8 (C-H $\cdots\pi$) | -94.06 | 0.09 | -0.10 | 0.00 | -94.15 | 100.10 | 2.55 | 0.00 | 0.00 | 0.00 |
| Tet19 | D1 (HB)+D2 ($\pi\cdots\pi$)+D5 (HB) | -90.64 | -4.65 | 5.13 | 0.13 | -57.95 | 63.94 | 1.57 | -28.04 | 30.94 | 0.76 |
| Tet20 | 2D2 ($\pi\cdots\pi$)+D3 (HB)+D6 (HB) | -90.08 | -2.72 | 3.02 | 0.07 | -31.28 | 34.73 | 0.85 | -56.08 | 62.26 | 1.52 |
| Tet21 | D1 (HB)+D3 (HB)+D6 (HB)+D4 (HB) | -89.10 | 0.14 | -0.15 | 0.00 | -89.23 | 100.15 | 2.41 | 0.00 | 0.00 | 0.00 |
| Tet22 | 2D2 ($\pi\cdots\pi$)+D3 (HB)+D6 (HB) | -88.82 | -1.46 | 1.65 | 0.04 | -31.28 | 35.22 | 0.85 | -56.08 | 63.14 | 1.52 |
| Tet23 | D1 (HB)+2D3 (HB) | -87.93 | -3.98 | 4.52 | 0.11 | -83.96 | 95.48 | 2.27 | 0.00 | 0.00 | 0.00 |
| Tet24 | D1 (HB)+D3 (HB)+D5 (HB) +D8 (HB) | -86.27 | -2.68 | 3.11 | 0.07 | -83.59 | 96.89 | 2.26 | 0.00 | 0.00 | 0.00 |
| Tet25 | 2D2 ($\pi\cdots\pi$)+D5 (HB)+D4 (HB) | -85.73 | -2.15 | 2.50 | 0.06 | -27.51 | 32.09 | 0.74 | -56.08 | 65.41 | 1.52 |
| Tet26 | D2 ($\pi\cdots\pi$)+D3 (HB)+D5 (HB)+D6 (HB)+D4 (HB) | -85.56 | 1.28 | -1.49 | -0.03 | -58.79 | 68.72 | 1.59 | -28.04 | 32.77 | 0.76 |
| Tet27 | D1 (HB)+D3 (HB)+D4 (HB)+D7 (HB) | -85.27 | -0.13 | 0.16 | 0.00 | -85.14 | 99.85 | 2.30 | 0.00 | 0.00 | 0.00 |
| Tet28 | 3D2 ($\pi\cdots\pi$) | -84.99 | -0.88 | 1.03 | 0.02 | 0.88 | -1.03 | -0.02 | -84.99 | 100.00 | 2.30 |
| Tet29 | D1 (HB)+2D3 (HB) | -84.11 | -0.15 | 0.18 | 0.00 | -83.96 | 99.82 | 2.27 | 0.00 | 0.00 | 0.00 |
| Tet30 | D1 (HB)+2D3 (HB) | -83.86 | 0.10 | -0.12 | 0.00 | -83.96 | 100.12 | 2.27 | 0.00 | 0.00 | 0.00 |
| Tet31 | D1 (HB)+D3 (HB)+D5 (HB) | -81.09 | -3.26 | 4.03 | 0.09 | -77.83 | 95.98 | 2.10 | 0.00 | 0.00 | 0.00 |
| Tet32 | D2 ($\pi\cdots\pi$)+2D3 (HB)+D6 (HB) | -80.49 | -1.29 | 1.60 | 0.04 | -51.16 | 63.57 | 1.38 | -28.04 | 34.84 | 0.76 |
| Tet33 | D2 (HB)+D3 (HB)+D5 (HB)+D4 (HB) | -76.35 | -0.93 | 1.21 | 0.03 | -75.43 | 98.79 | 2.04 | 0.00 | 0.00 | 0.00 |
| Tet34 | D1 (HB)+2D5 (HB) | -70.26 | 1.45 | -2.06 | -0.04 | -71.71 | 102.06 | 1.94 | 0.00 | 0.00 | 0.00 |
| Tet35 | D3 (HB)+2D5 (HB)+D6 (HB) +D8 (HB) | -64.29 | 0.26 | -0.40 | -0.01 | -64.55 | 100.40 | 1.75 | 0.00 | 0.00 | 0.00 |
| Tet36 | D3 (HB)+2D5 (HB)+D6 (HB) +D8 (HB) | -64.15 | 0.40 | -0.62 | -0.01 | -64.55 | 100.62 | 1.75 | 0.00 | 0.00 | 0.00 |
| Tet37 | 2D3 (HB)+D4 (HB)+D7 (C-H $\cdots\pi$) | -60.76 | 0.07 | -0.11 | 0.00 | -60.82 | 100.11 | 1.64 | 0.00 | 0.00 | 0.00 |
| Tet38 | 3D3 (HB) | -59.36 | 0.28 | -0.46 | -0.01 | -59.64 | 100.46 | 1.61 | 0.00 | 0.00 | 0.00 |
| Tet39 | D3 (HB)+D6 (HB)+D4 (HB)+D7 (HB)+D8 (HB) | -58.52 | -0.42 | 0.71 | 0.01 | -58.11 | 99.29 | 1.57 | 0.00 | 0.00 | 0.00 |
| Tet40 | D3 (HB)+D5 (HB)+D6 (HB)+D7 (HB) | -51.84 | 0.51 | -0.98 | -0.01 | -52.35 | 100.98 | 1.42 | 0.00 | 0.00 | 0.00 |
| Σ^* | | | | | 1.04 | | | 75.45 | | | 23.52 |

*The summation of the percentage of weighted contribution of E_{coop} , E_{HB} and $E_{\pi\cdots\pi}$ in all of the tetramer fragments

Table S2. The binding energy (E_{calc} in kJ/mol) of the most stable tetramer fragments of compound *II*, along with contribution of cooperativity (E_{coop}), HB (E_{HB}) and $\pi \dots \pi$ stacking ($E_{\pi \dots \pi}$) energies as the magnitude (in kJ/mol) and percentage of total binding energy, as well as their weighted contributions.

| Thiophene | E_{calc} | E_{coop} | % E_{coop} | %W E_{coop} | E_{HB} | %HB | %WH B | $E_{\pi\text{-based}}$ | % $\pi\text{-based}$ | %W $\pi\text{-based}$ | |
|--------------|--|-------------------|---------------------|-------------------------|-----------------|--------|----------|------------------------|----------------------|-----------------------|--------------|
| Tet1 | 2D1 ($\pi \dots \pi$)+D2 (HB)+D5 (HB)+D7 (HB)+D9 (HB) | -140.76 | -2.39 | 1.70 | 0.06 | -59.49 | 42.26 | 1.55 | -78.88 | 56.04 | 2.06 |
| Tet2 | D1 ($\pi \dots \pi$)+2D2 (HB)+D5 (HB)+D6 ($\pi \dots \pi$)+D7 (HB) | -140.30 | -3.55 | 2.53 | 0.09 | -86.96 | 61.98 | 2.27 | -49.79 | 35.49 | 1.30 |
| Tet3 | D1 ($\pi \dots \pi$)+2D2 (HB)+D5 (HB)+D6 ($\pi \dots \pi$)+D7 (HB) | -140.27 | -3.52 | 2.51 | 0.09 | -86.96 | 62.00 | 2.27 | -49.79 | 35.50 | 1.30 |
| Tet4 | D1 ($\pi \dots \pi$)+2D2 (HB)+2D5 (HB) | -134.71 | -3.58 | 2.66 | 0.09 | -91.68 | 68.06 | 2.39 | -39.44 | 29.28 | 1.03 |
| Tet5 | D1 ($\pi \dots \pi$)+2D2 (HB)+ D5 (HB) | -120.48 | -3.13 | 2.60 | 0.08 | -77.91 | 64.67 | 2.03 | -39.44 | 32.74 | 1.03 |
| Tet6 | D1 ($\pi \dots \pi$)+D2 (HB)+D3 ($\pi \dots \pi$)+D4 (HB) +D8 (HB) | -119.78 | 1.03 | -0.86 | -0.03 | -53.99 | 45.07 | 1.41 | -66.82 | 55.79 | 1.74 |
| Tet7 | D1 ($\pi \dots \pi$)+ D2 (HB)+ D3 ($\pi \dots \pi$)+D5 (HB) | -113.26 | -0.58 | 0.51 | 0.02 | -11.48 | 10.14 | 0.30 | -101.19 | 89.35 | 2.64 |
| Tet8 | D1 ($\pi \dots \pi$)+D2 (HB)+2D5 (HB)+D6 ($\pi \dots \pi$) | -111.82 | -2.40 | 2.15 | 0.06 | -59.63 | 53.33 | 1.56 | -49.79 | 44.53 | 1.30 |
| Tet9 | 2D2 (HB)+D3 ($\pi \dots \pi$)+D4 (HB) | -110.25 | -3.04 | 2.76 | 0.08 | -79.82 | 72.41 | 2.08 | -27.38 | 24.83 | 0.71 |
| Tet10 | D2 (HB)+D2 (HB)+D3 ($\pi \dots \pi$)+D4 (HB) | -109.10 | -1.90 | 1.74 | 0.05 | -79.82 | 73.17 | 2.08 | -27.38 | 25.10 | 0.71 |
| Tet11 | D1 ($\pi \dots \pi$)+D2 (HB)+D3 ($\pi \dots \pi$)+D7 (HB) | -109.01 | -1.06 | 0.97 | 0.03 | -41.14 | 37.74 | 1.07 | -66.82 | 61.30 | 1.74 |
| Tet12 | D2 (HB)+2D3 ($\pi \dots \pi$)+D4 (HB)+D9 (HB) | -106.88 | 0.19 | -0.18 | -0.01 | -52.32 | 48.95 | 1.37 | -54.76 | 51.23 | 1.43 |
| Tet13 | 2D1 ($\pi \dots \pi$)+D3 ($\pi \dots \pi$) | -106.56 | -0.30 | 0.28 | 0.01 | 0.30 | -0.28 | -0.01 | -106.56 | 100.00 | 2.78 |
| Tet14 | D1 ($\pi \dots \pi$)+D2 (HB)+2D5 (HB)+D9 (HB) | -104.32 | -0.70 | 0.67 | 0.02 | -64.18 | 61.52 | 1.68 | -39.44 | 37.81 | 1.03 |
| Tet15 | D1 ($\pi \dots \pi$)+D2 (HB)+D4 (HB)+D5 (HB) | -103.10 | -2.15 | 2.08 | 0.06 | -61.51 | 59.66 | 1.61 | -39.44 | 38.26 | 1.03 |
| Tet16 | 2D2 (HB)+2D5 (HB)+D6 ($\pi \dots \pi$) | -102.53 | -0.50 | 0.49 | 0.01 | -91.68 | 89.42 | 2.39 | -10.35 | 10.09 | 0.27 |
| Tet17 | 3D2 (HB) | -102.00 | -5.80 | 5.69 | 0.15 | -96.20 | 94.31 | 2.51 | 0.00 | 0.00 | 0.00 |
| Tet18 | D1 ($\pi \dots \pi$)+D3 ($\pi \dots \pi$)+D4 (HB)+D5 (HB)+D9 (HB) | -100.77 | 0.05 | -0.05 | 0.00 | -34.00 | 33.74 | 0.89 | -66.82 | 66.31 | 1.74 |
| Tet19 | D1 ($\pi \dots \pi$)+D2 (HB)+D4 (HB)+D5 (HB) | -100.69 | 0.29 | -0.29 | -0.01 | -61.54 | 61.12 | 1.61 | -39.44 | 39.17 | 1.03 |
| Tet20 | 2D2 (HB)+D5 (HB)+D6 ($\pi \dots \pi$)+D7 (HB) | -100.29 | -2.94 | 2.94 | 0.08 | -86.99 | 86.75 | 2.27 | -10.35 | 10.32 | 0.27 |
| Tet21 | D2 (HB)+D3 ($\pi \dots \pi$)+D4 (HB)+D5 (HB)+D6 ($\pi \dots \pi$) | -97.75 | 1.48 | -1.51 | -0.04 | -61.51 | 62.92 | 1.61 | -37.73 | 38.59 | 0.99 |
| Tet22 | D1 ($\pi \dots \pi$)+2D3 ($\pi \dots \pi$) | -94.03 | 0.17 | -0.18 | 0.00 | -0.17 | 0.18 | 0.00 | -94.03 | 100.00 | 2.45 |
| Tet23 | D1 ($\pi \dots \pi$)+D2 (HB)+D5 (HB)+D9 (HB) | -90.97 | -1.16 | 1.27 | 0.03 | -50.37 | 55.37 | 1.32 | -39.44 | 43.36 | 1.03 |
| Tet24 | 2D1 ($\pi \dots \pi$)+D6 ($\pi \dots \pi$) | -90.22 | -0.99 | 1.10 | 0.03 | 0.99 | -1.10 | -0.03 | -90.22 | 100.00 | 2.36 |
| Tet25 | D1 ($\pi \dots \pi$)+D3 ($\pi \dots \pi$)+D4 (HB)+D8 (HB) | -89.22 | -0.47 | 0.53 | 0.01 | -21.93 | 24.58 | 0.57 | -66.82 | 74.89 | 1.74 |
| Tet26 | D1 ($\pi \dots \pi$)+D3 ($\pi \dots \pi$)+D5 (HB) +D9 (HB) | -85.13 | 0.01 | -0.01 | 0.00 | -18.32 | 21.52 | 0.48 | -66.82 | 78.49 | 1.74 |
| Tet27 | D2 (HB)+D4 (HB)+D5 (HB)+D6 ($\pi \dots \pi$)+D8 (HB) | -79.53 | -1.42 | 1.79 | 0.04 | -67.76 | 85.20 | 1.77 | -10.35 | 13.01 | 0.27 |
| Tet28 | D1 ($\pi \dots \pi$)+D4 (HB)+D5 (HB)+D8 (HB)+D9 (HB) | -79.49 | 0.21 | -0.26 | -0.01 | -40.25 | 50.64 | 1.05 | -39.44 | 49.62 | 1.03 |
| Tet29 | 2D2 (HB)+D4 (HB) | -79.25 | 0.58 | -0.73 | -0.02 | -79.82 | 100.73 | 2.08 | 0.00 | 0.00 | 0.00 |
| Tet30 | 2D2 (HB)+D5 (HB) | -79.06 | -1.15 | 1.46 | 0.03 | -77.91 | 98.54 | 2.03 | 0.00 | 0.00 | 0.00 |
| Tet31 | D1 ($\pi \dots \pi$)+D3 ($\pi \dots \pi$)+D6 ($\pi \dots \pi$) | -77.91 | -0.75 | 0.96 | 0.02 | 0.75 | -0.96 | -0.02 | -77.91 | 100.00 | 2.03 |
| Tet32 | D1 ($\pi \dots \pi$)+D3 ($\pi \dots \pi$)+D6 ($\pi \dots \pi$) | -76.56 | 0.61 | -0.80 | -0.02 | -0.61 | 0.80 | 0.02 | -76.56 | 100.00 | 2.00 |
| Tet33 | D2 (HB)+D5 (HB)+2D6 ($\pi \dots \pi$)+D7 (HB) | -76.24 | -0.64 | 0.84 | 0.02 | -54.91 | 72.01 | 1.43 | -20.70 | 27.15 | 0.54 |
| Tet34 | D1 ($\pi \dots \pi$)+D3 ($\pi \dots \pi$)+D6 ($\pi \dots \pi$) | -76.16 | 1.01 | -1.32 | -0.03 | -1.01 | 1.32 | 0.03 | -76.16 | 100.00 | 1.99 |
| Tet35 | D2 (HB)+D4 (HB)+D5 (HB)+D6 ($\pi \dots \pi$) | -71.70 | 0.16 | -0.23 | 0.00 | -61.51 | 85.79 | 1.61 | -10.35 | 14.43 | 0.27 |
| Tet36 | D2 (HB)+2D5 (HB)+D6 ($\pi \dots \pi$) | -71.00 | -1.06 | 1.49 | 0.03 | -59.60 | 83.94 | 1.56 | -10.35 | 14.58 | 0.27 |
| Tet37 | D1 ($\pi \dots \pi$)+D5 (HB)+D6 ($\pi \dots \pi$)+D9 (HB) | -67.67 | 0.44 | -0.65 | -0.01 | -18.32 | 27.07 | 0.48 | -49.79 | 73.58 | 1.30 |
| Tet38 | D3 ($\pi \dots \pi$)+D4 (HB)+D6 ($\pi \dots \pi$)+D8 (HB)+D9 (HB) | -64.29 | -0.08 | 0.12 | 0.00 | -26.48 | 41.19 | 0.69 | -37.73 | 58.69 | 0.99 |
| Tet39 | 2D3 ($\pi \dots \pi$)+D6 ($\pi \dots \pi$) | -62.80 | 2.31 | -3.67 | -0.06 | -2.31 | 3.67 | 0.06 | -62.80 | 100.00 | 1.64 |
| Tet40 | D3 ($\pi \dots \pi$)+2D6 ($\pi \dots \pi$) | -46.04 | 2.03 | -4.42 | -0.05 | -2.03 | 4.42 | 0.05 | -46.04 | 100.00 | 1.20 |
| Σ^* | | | | | 0.91 | | | 50.11 | | | 48.99 |

* The summation of the percentage of weighted contribution of E_{coop} , E_{HB} and $E_{\pi \dots \pi}$ in all of the tetramer fragments